NASA TECHNICAL NOTE

NASA TN D-2040

NASA TN D-2040

A STUDY OF SEVERAL OXIDATION-RESISTANT COATINGS ON Mo-0.5Ti ALLOY SHEET AT 2,500° F

by Donald R. Rummler, Bland A. Stein, and Richard A. Pride

Langley Research Center
Langley Station, Hampton, Va.

NATIONAL AERONAUTICS AND SPACE ADMINISTRATION • WASHINGTON, D. C. • AUGUST 1964

56961

A STUDY OF SEVERAL OXIDATION-RESISTANT COATINGS ON Mo-0.5Ti ALLOY SHEET AT 2,500° F

By Donald R. Rummler, Bland A. Stein,
and Richard A. Pride

Langley Research Center
Langley Station, Hampton, Va.

NATIONAL AERONAUTICS AND SPACE ADMINISTRATION

For sale by the Office of Technical Services, Department of Commerce,
Washington, D.C. 20230 -- Price $2.00

A STUDY OF SEVERAL OXIDATION-RESISTANT COATINGS ON Mo-0.5Ti ALLOY SHEET AT 2,500° F

By Donald R. Rummler, Bland A. Stein, and Richard A. Pride

SUMMARY

The results are presented of a study of several silicide-base oxidation-resistant coatings applied to 0.012-inch-thick molybdenum-alloy sheet. The specimens were both continuously and cyclically exposed at 2,500° F in air. The effect of three different types of thermal cycles was investigated. A failure mechanism is proposed to explain the severe reduction observed in the ability of a coating to protect the substrate when thermally cycled. A failure mechanism for the continuously exposed coated specimens is also proposed. The investigation includes the results of X-ray studies and room-temperature mechanical-property tests on the coated specimens.

INTRODUCTION

Molybdenum-base alloys have been considered for use as heat shields in the thermal-protection systems contemplated for several aerospace vehicles. The heat shields of these vehicles will be subjected to temperatures above 2,000° F for extended periods of time. In addition, the more advanced of these vehicles will be expected to perform multiple exits and reentries with a minimum of rework between flights.

Two of the major problems associated with the use of molybdenum alloys in this application are: (1) poor oxidation resistance at high temperatures which requires the use of a protective coating, and (2) high density which requires that these alloys be utilized in thin gages.

The development of oxidation-resistant coatings for molybdenum alloys has received considerable attention. (See, for example, refs. 1 to 4.) Although considerable progress has been made to develop a reliable coating to protect molybdenum-base alloys, major problem areas still exist. Two of the most important of these areas are: (1) the tendency of coatings to fail initially on the edges, particularly in thin-gage material, and (2) the severe reduction of coating performance when subjected to thermal cycling.

In order to assess the progress which has been made in the development of a reliable oxidation-resistant coating system for molybdenum-alloy sheet, a study

was undertaken to evaluate several coatings applied to 0.012-inch-thick Mo-0.5Ti sheet under a variety of test conditions. Special emphasis was placed on edge failures and the effects of thermal cycling.

The program included both continuous- and cyclic-exposure oxidation tests at 2,500° F in air. The oxidation resistance of specimens with three different edge preparations was studied. Three different cyclic-exposure tests were included to determine the effects of heating rate and time at test temperature on the oxidation resistance of the coatings. The program also included room-temperature tensile tests and metallurgical and X-ray investigations on the coated specimens.

Some preliminary results of this investigation are presented in reference 5. The investigation reported in reference 6 was concurrent with this program and contains additional information on the effects of high-temperature exposure on coated molybdenum-alloy sheet.

SYMBOLS AND NOTATION

A(G)	coating A, preglassed
E	Young's modulus
El	elongation in 2 inches, percent
W	as-coated specimen weight
ΔW	change in specimen weight
ϵ	strain
σ	stress
σ_{tu}	ultimate tensile strength
σ_{ty}	0.2-percent offset tensile yield strength

Subscript:

o	before coating

SPECIMENS

Fabrication

The specimens in this study consisted of three types of oxidation tabs and small tensile specimens. All the specimens were fabricated from stress-relieved-molybdenum—0.5-percent-titanium sheet (Mo-0.5Ti), nominally 0.012 inch thick. In order to investigate the effect of substrate edge preparation on coating performance, the oxidation tabs were fabricated with one of the following edge conditions:

(1) Sheared to $1\frac{5}{8} \times \frac{7}{8}$ inches at temperatures of approximately 200° to 300° F

(2) Machined to $1\frac{1}{2} \times \frac{3}{4}$ inches; edges deburred by hand with emery

(3) Machined to $1\frac{1}{2} \times \frac{3}{4}$ inches with 0.125-inch radii at corners; dry tumbled in an abrasive mix containing No. 180 silicon carbide grit and rounded pebbles

These three edge conditions will hereinafter be referred to as sheared, broken, and tumbled edges, respectively.

The edge preparations produced three distinctly different edge conditions on the Mo-0.5Ti substrate which are shown in cross section in figure 1. The sheared edge (fig. 1(a)) indicates that considerable plastic deformation of the substrate material occurred during the shearing operation. The broken edge (fig. 1(b)) has a slight radius at the corners due to the deburring. The generous continuous radius of the tumbled-edge specimen in figure 1(c) indicates that this preparation method is the most suitable for the elimination of sharp angles which may foster uneven deposition of the coating.

The tensile specimens were 6 inches long and 0.50 inch wide with a 4-inch gage section reduced to 0.375 inch. The tensile specimens were sheared at temperatures from 200° to 300° F and then machined to finished size. The tensile specimens received no additional edge preparation by the NASA prior to shipment to the coating suppliers.

Coatings

The specimens were all fabricated by NASA, individually measured and weighed, and then forwarded to various coating suppliers for the application of a coating. The coatings selected for this study were all silicide based. The selected coatings and methods of application are listed in table I. Detailed descriptions of the pack-cementation and fluidized-bed coating processes can be found in references 1 to 3. Only one of the coatings supplied, coating B, was an unmodified silicide coating. Table I also lists the constituents which were added to the pack to modify the other coatings. References are included for additional information.

The specifications for the coatings were intended to furnish guidelines for the coating which would represent the best compromise between maximum oxidation protection and minimum alteration of the mechanical properties of the uncoated molybdenum-alloy substrate. The suggested guidelines given to the coating suppliers included the following:

(1) Oxidation resistance of at least 10 hours at 2,500° F in static air

(2) A maximum allowable decrease in room-temperature elongation of 25 percent

(3) A maximum allowable weight increase of 25 percent

In addition to the performance guides, the coating supplier was requested to apply the same coating to all specimens and to use his normal cleaning and surface preparation procedures prior to coating. The coated specimens were received from the various coating suppliers between July and December of 1961. The only obvious detrimental effect of the coating procedures was warpage observed in some of the tensile specimens. The thickness and weight of each coated specimen were determined and the overall appearance of specimens with each coating was noted.

Typical oxidation tabs were then selected for microscopic examination to determine the thickness of the coating and substrate. Table II presents measurements of the tumbled-edge oxidation specimens before and after coating and includes average coating thickness, substrate thickness before and after coating, and the average weight gain for each coating supplied. Although the data presented in table II were obtained from tumbled-edge oxidation specimens only, they are considered typical of the coating included in this evaluation since the specimens were either coated as a single lot or were coated in batches which contained a mixture of specimens with two or more edge conditions.

The weight change as a result of coating application represents the average change in weight of the tumbled-edge specimens which were supplied to each coating supplier. This weight change includes the effects of any surface removal of the substrate by the coating supplier prior to coating. Specimens with coating B, for instance, showed a net weight loss after coating which was due primarily to surface preparation and not to the suspension holes which were drilled in the specimens to facilitate coating in the fluidized-bed process.

EQUIPMENT AND PROCEDURES

Metallurgical Examination

The metallurgical examination consisted of (1) macroscopic and metallographic examination of as-coated specimens, (2) X-ray diffraction studies of as-coated and tested oxidation specimens, and (3) X-ray emission studies of as-coated and tested specimens.

Specimens representative of each coating were sectioned, mounted, polished, and etched as described in reference 6 prior to examination with the light microscope. It was believed that such an examination of coating cross section would be

helpful in pointing out differences in the structure of the coatings under investigation and in explaining coating performance in the oxidation tests.

The surfaces of both as-coated and tested specimens were examined by X-ray diffraction with a diffractometer to determine the constituents present. Nickel-filtered copper K_α radiation was used for the diffraction studies. The depth of X-ray penetration was calculated by assuming the surface to be $MoSi_2$ and using the information presented in reference 7. These calculations indicated that 90 percent of the information on a diffraction pattern obtained from examination of a coated surface was obtained from approximately the first 0.0002 inch of the surface.

The surface of both as-coated and tested specimens was also examined by X-ray emission techniques. Both platinum K_α and chromium K_α radiation were used.

Oxidation Tests

The types of oxidation tests utilized in this investigation are indicated in figure 2. During the constant-temperature tests, oxidation specimens were exposed to the test temperature in a vertical tube furnace. The weight change of the specimens was continuously monitored with the aid of an automatic recording balance. When specimen weight loss exceeded 10 percent, the test was usually terminated. Specimens which did not experience a weight loss of 10 percent within 250 hours were usually removed from the furnace. Additional details of the equipment and procedures used for this test are presented in appendix A.

In both the 0.1-hour and the 1.0-hour cyclic tests (fig. 2), the specimens were rapidly inserted into a muffle furnace which achieved 95 percent of the temperature change in 30 seconds. At the completion of the cycle, the specimens were allowed to air-cool. During the other 1.0-hour cyclic test, the test specimen was heated at a slow, linear temperature-rise rate which was designed to bring the specimen to the test temperature of 2,500° F in 0.5 hour. The specimen was exposed to the test temperature for 1 hour and then was cooled at a controlled rate which resulted in a linear temperature decrease for 0.5 hour back to room temperature. This cycle will hereinafter be referred to as the 0.5-1.0-0.5—hour cycle. In the cyclic oxidation tests, the specimens were weighed after each cycle and the tests were terminated after a 10-percent weight loss. A detailed description of the equipment and procedures used for the cyclic tests is presented in appendix B.

Appendix C compares the results of continuous oxidation tests performed in the vertical tube and the muffle furnaces on both bare and coated molybdenum specimens.

Tensile Tests

Tensile stress-strain tests were performed at room temperature on the 120,000-pound-capacity universal hydraulic testing machine at the Langley Research Center at a nominal strain rate of 0.005 per minute to yield and 0.050 per minute from yield to failure. Strain rates were controlled by continuously monitoring

head motion during the test. Strains were measured by using optical strain gages attached on both sides of the specimen; strains were read while the strain rate was maintained. Elongation measurements were made by using finely scribed pencil lines at 1/4-inch intervals along the specimens.

RESULTS AND DISCUSSION

Metallurgical Investigation

Metallography.- The macroscopic and metallographic examinations were conducted on specimens in the as-coated condition. Additional information on the substrate properties is presented in reference 6. The alphabetic symbols which appear in the photomicrographs are for identification of phase separation and are not intended to identify phases which are common to the coatings. No rigorous attempt was made to identify all the phases which were present in the various coatings, and it is recognized that in some coatings additional phases are required to preserve stoichiometry.

Coating A: Coating A is a highly modified silicide-based coating applied by pack cementation. The as-coated appearance of the specimens consisted of a dull gray, matted surface which was speckled with spots of darker gray (fig. 3(a)). A photomicrograph of a cross section of the specimen indicates that the coating in the as-coated condition contained three distinct phases (fig. 3(b)). Under polarized light (fig. 3(c)), the thick outside layer (a) is active and shows a columnar structure which is common for a vapor-deposition process.

Activity under polarized light is reported to be a property of $MoSi_2$ (ref. 8). The barely visible layer (b), which appears next to the $MoSi_2$, does not appear to be active under polarized light. In reference 6 this phase was identified as Mo_3Si. Adjacent to this layer is a somewhat thicker dark phase (c) which shows no grain structure with the etchant used and has a pronounced diffusion boundary with the molybdenum substrate. This phase, $Mo_5(B,Si)_3$, contains boron and is discussed in reference 6.

Coating A(G): The specimens with coating A(G) are the same as the unglassed coating A specimens with an additional treatment by the coating supplier. In this treatment, the specimens were exposed to an oxidizing atmosphere of reduced oxygen partial pressure at 2,800° F. The intent of this treatment was to insure an oxide formation on the outer surface of the coating and consequently to provide a more reliable protection for the substrate. The appearance of the coating A(G) specimens (fig. 4(a)) after coating was the same dull gray with dark spots seen on the coating A specimens but with a surface glaze which indicated that the additional oxidizing cycle had produced some form of glassy oxide. When examined microscopically in cross section under bright light (fig. 4(b)), the coating appeared to be composed of three distinct phases. The thick outer phase (a) was slightly attacked by the etchant and exhibited a columnar structure, indicating $MoSi_2$. Adjacent to the outer phase was a phase (b) which appeared as

a light band and did not reveal a grain structure. This phase (b) was identified in reference 6 as Mo_5Si_3. Next to this phase was a thin, almost black band (c), $Mo_5(B,Si)_3$ (ref. 6), which appeared to have no grain structure, was not of uniform thickness, and was bounded on both sides by sharply defined diffusion boundaries. Polarized lighting of the magnified cross section (fig. 4(c)) confirmed the columnar structure of the outer phase. In addition, the outer phase appeared to have a more equiaxed orientation of the grains near the surface of the coating.

Coating B: A notable feature of the as-coated oxidation tabs with coating B (fig. 5(a)) was the hole drilled and chamfered by the supplier to facilitate coating in the fluidized-bed process. Coating B was the only coating in the present study applied by this method. The appearance of the coating B specimens was the most uniform of those investigated and was dull gray with a matte texture. This coating was also the only coating investigated which is reported to be a pure disilicide (ref. 1). When examined under bright light in cross section (fig. 5(b)), the coating revealed only one phase (a) which was uniform in thickness. Examination under polarized light (fig. 5(c)) clearly indicates at least one effect of the fluidized-bed process. The $MoSi_2$ grain structure was random and did not have the preferential columnar structure which was characteristic of the coatings which were applied by the more conventional pack-cementation process. The supplier did not coat the as-sheared specimens which were provided.

Coating C: The typical as-coated appearance of coating C (fig. 6(a)), although a highly modified disilicide coating, was characteristically dull gray with a matte texture. Some uneveness of color was noted near the edges but none of the specimens had the mottled appearance of other modified coatings. When examined under bright light, a cross-sectioned specimen (fig. 6(b)) appeared to contain only two phases (a and b). However, when examined under polarized light (fig. 6(c)), the outer phase (a) contained two distinct grain structures (a and a'). Although both are columnar in form, the grain structure on the outer surface (a) consisted of larger grains which were less severely oriented than the inner grain structure (a'). Although it is not clearly apparent in the photomicrograph, the appearance of these two grain structures under polarized light differs considerably from that of the other coatings. In all the other coatings, the phase which was optically active under polarized light (assumed to be $MoSi_2$) appeared to be composed of varying shades of bluish gray. In coating C this phase was made up of various shades of pink and light gray. This coloring may be due to the $Mo(Al,Si)_2$ which was identified on the surface of the coating by X-ray diffraction. Although different in appearance, the two grain structures (a and a') exhibited the same Knoop hardness (ref. 6). There was also a thin phase (b) next to the molybdenum substrate which was not active under polarized light and revealed no grain structure with the etchant used. Coating C was the thinnest and most nonuniform of the coatings investigated.

Coating D: Coating D is a chrome-modified silicide coating. The as-coated appearance of this coating is presented in figure 7(a). The coating was typically matte gray with many small spots of lighter and darker gray. On some specimens the edges were rough and appeared to be discontinuous. When a sectioned specimen was examined under bright light (fig. 7(b)), the coating revealed only one phase and no distinct grain pattern with the etchant used. The coating-metal interface was

clearly defined. Examination under polarized light (fig. 7(c)) revealed the characteristic columnar structure of coatings deposited by pack cementation. The high optical activity of the coating indicated that $MoSi_2$ was the major constituent of the coating.

Coating E: Coating E was mottled gray in color and exhibited the roughest surface texture of the coatings supplied (fig. 8(a)). All the broken-edge and sheared-edge specimens which were provided to the supplier for coating applications received additional edge treatment. The edges and corners were rounded abrasively and, as a result, oxidation data presented for the coated broken-edge and sheared-edge specimens are of questionable value for comparing the effects of the different edge conditions. When this coating was cross sectioned and examined under bright light (fig. 8(b)), it was found to contain three distinct phases. The dark outer layer (a) appeared to be dense and showed no grain structure. When examined under polarized light (fig. 8(c)), it was apparent that the outer phase (a) was not just a porous form of the $MoSi_2$. The second phase (b) exhibited the columnar, optically active, structure of $MoSi_2$ when deposited by pack cementation.

Coating F: As was noted for coating E, coating F broken-edge and sheared-edge specimens were given additional edge treatment prior to coating by the coating supplier. The coating surface was mottled dull gray with a matte texture (fig. 9(a)). Coating F under bright light and in cross section (fig. 9(b)) was uniform in thickness. The etchant used revealed a two-phase system similar to the other two-phase coatings. Under polarized light (fig. 9(c)), the optically active $MoSi_2$ made up the major portion of the coating (a). A thin phase (b) which is assumed to be Mo_5Si_3 separated the $MoSi_2$ from the substrate. This thin phase, as in the other coatings, showed no grain structure.

X-ray diffraction.- In order to provide a more complete understanding of the protection and failure mechanisms which were operative in the silicide-based coatings tested, a detailed X-ray investigation was undertaken to identify the various elements and/or compounds presented on the surface of the various coatings. Specimens were selected from each coating in the as-coated condition and after failure in both the continuous-exposure and cyclic-exposure tests.

Coating A: $MoSi_2$ was found to be the major constituent on the surface of the as-coated specimens with coating A. Although coating A had numerous elements added to the pack to modify the coating, X-ray diffraction examination of the as-coated specimens indicated only boron in addition to the silicon in the coating. Boron was detected in the compound $Mo_5(B,Si)_3$; Mo_5Si_3 and α quartz were also detected on the surface of the as-coated specimens. After exposure to fifteen 1-hour cycles of 2,500° F, the major constituent was still $MoSi_2$. The $Mo_5(B,Si)_3$ and α quartz were not detected. Alpha cristobalite, Mo_3Si, and Mo_5Si_3 were also identified. After 264 hours of continuous exposure, X-ray diffraction of the coated surface revealed only Mo_5Si_3 and Mo_3Si in significant quantities. No $MoSi_2$ was detected. Although the crystalline α cristobalite was not found, the X-ray pattern exhibited a broad peak or hump similar to the broad peak which is reported in reference 9 as the absence of small-angle scattering and a characteristic of vitreous silica. Examination of specimen 33 (table V), which failed in

0.4 hour, revealed α cristobalite on the surface, accompanied by a white crystalline appearance, in addition to Mo_5Si_3 and Mo_3Si.

Coating A(G): The specimens with coating A(G) received an additional oxidizing cycle at 2,800° F before delivery as discussed previously. The surface of the as-coated specimens was composed primarily of $MoSi_2$ with both Mo_5Si_3 and α cristobalite also present. After thirty-six 1-hour cycles, $MoSi_2$ was still the major constituent; Mo_5Si_3, Mo_3Si, and α cristobalite were also detected. Examination of the coating A(G) specimens after 167 hours of continuous exposure revealed Mo_5Si_3 and Mo_3Si with some α cristobalite and $MoSi_2$ also present.

Coating B: Coating B was the only coating supplied which is reported to contain no additives. On the as-coated surface only $MoSi_2$ was found by X-ray diffraction techniques. After nine 1-hour cycles, $MoSi_2$ was still the major constituent of the surface; Mo_5Si_3, and Mo_3Si, and α cristobalite were also detected. After 20.5 hours of continuous exposure, the surface was composed of α crystobalite and $MoSi_2$; some Mo_5Si_3 and Mo_3Si were also detected.

Coating C: The major constituent on the surface of the as-coated specimens with coating C was identified as $Mo(Si,Al)_2$; α Al_2O_3 and α cristobalite were also detected by X-ray diffraction examination of the as-coated surface. After exposure to three 1.0-hour cycles, α Al_2O_3 was present as the major constituent, with some Mo_5Si_3, Mo_3Si, and $MoSi_2$ also present. No $Mo(Si,Al)_2$ or α cristobalite was detected. A specimen continuously exposed for 4.7 hours was examined and found to contain α Al_2O_3 and Mo_5Si_3 as the major compounds with some $MoSi_3$, α cristobalite, $MoSi_2$, and Mo_3Si also detected. The coated surface showed no appreciable change in the relative amounts of the four compounds identified after 4.7 hours when it was continuously exposed for 24.2 hours.

Coating D: The as-coated surface of the specimens with coating D was found to be primarily $MoSi_2$ with some Mo_5Si_3. After three 0.1-hour cycles the surface was still primarily $MoSi_2$; some α cristobalite and Mo_5Si_3 were also noted. After four 1.0-hour cycles the surface was primarily $MoSi_2$ with some α cristobalite and Mo_5Si_3. After continuous exposure for 18.4 hours, the major constituent was α cristobalite; some $MoSi_2$, Mo_5Si_3, and Mo_3Si were also detected.

Coating E: Coating E was applied in a two-cycle pack cementation; the first cycle was a chromizing treatment and the second cycle, the typical siliconizing process. The surface of the as-coated specimens was composed primarily of $MoSi_2$; Al_2O_3, α quartz, and Cr_2O_3 were also detected. After ten 0.1-hour cycles, the coating surface contained α cristobalite and Cr_2O_3, and detectable percentages of α quartz and $MoSi_2$. When exposed to twenty-three 1-hour cycles, the surface

consisted primarily of α cristobalite and $MoSi_2$ with some Cr_2O_3, Mo_5Si_3, and Mo_3Si. After 66 hours of continuous exposure, the coating surface was almost entirely α cristobalite with Mo_5Si_3, Mo_3Si, and Cr_2O_3 also present.

Coating F: The small amount of columbium which was added to the pack powder of coating F to modify the coating was not detected by X-ray diffraction on the as-coated surface of this coating. The major constitutent was $MoSi_2$ on the as-coated surface with some α quartz also detected. When exposed to 2,500° F for twenty-five 1-hour cycles, the surface consisted primarily of Mo_5Si_3 with some α cristobalite, $MoSi_2$, and Mo_3Si. The percentages of both α cristobalite and Mo_3Si increased after 39.1 hours of continuous exposure with trace amounts of $MoSi_2$ and Mo_5Si_3 also present.

X-ray emission.- Examination of the as-coated specimens made by using X-ray emission techniques indicated that coating B was the only coating evaluated which did not contain a small amount of iron on the surface. The X-ray emission studies also indicated a small percentage of chromium in coating D and coating E. Both of these coatings reportedly contain chromium, but only coating E contained enough to be positively identified by X-ray diffraction techniques as Cr_2O_3.

Continuous-Exposure Oxidation Tests

Edge preparation is generally considered an important factor in coating performance on sheet material. Photomicrographs (fig. 10) of one of the coatings before exposure are typical of the as-coated appearance for the three edge conditions under investigation. As expected, the coating on the tumbled edge appears superior to the other two. The partially recrystallized substrate of the tumbled-edge and the sheared-edge specimens would suggest that these two edge preparations are less severe than the broken-edge preparation which resulted in a fully recrystallized substrate. The lower recrystallization temperature of the broken-edge specimen, which may be the result of a more severe fabrication process and the accompanying higher residual stresses, could contribute to a shorter life for a coating applied to this edge condition.

In order to evaluate more thoroughly the effect which edge preparation might have on the protection afforded the substrate by the various coatings, continuous-exposure oxidation tests were conducted. These tests subjected the coated oxidation tabs to a temperature of 2,500° F in slowly moving air. The results of these tests are presented separately for each type of edge condition.

Sheared edges.- Typical plots of weight change for coatings which were applied to sheared-edge tabs are shown in figure 11. It can be seen that all the coatings showed a weight loss during the first hour. The specimens with coating D generally showed a weight loss greater than 2 percent during the first hour. The loss of weight was usually accompanied by the evolution of smoke from the specimen. The smoking gradually stopped as the weight-loss rate decreased. The specimens would then usually remain at essentially the same weight for many hours before the

to 11

coating failed and the specimen catastrophically lost weight. Catastrophic weight loss was typical for all coatings applied to sheared-edged specimens. The one exception to this was coating A which characteristically exhibited a slow failure rate. A decrease in weight-loss rate or, in some cases, an abrupt small weight gain just prior to failure was noted for a majority of the specimens tested with sheared edges (fig. 11).

Because the constant-temperature tests were continuous, the initial point of coating breakdown was difficult to ascertain. Each specimen was examined after removal from the furnace and an attempt was made to determine the point of initial failure. The failures were judged either as an edge failure or as a general breakdown of the coating. Initial location of failure on the specimens was identified for 21 of the 24 specimens tested (table III). Of these, seven specimens failed initially on the edge. The apparent ability of coating E and coating F to protect against edge failure is suspect because of the previously noted additional edge treatment the specimens received.

The time for each sheared-edge specimen to sustain a weight loss of 2, 4, 6, 8, and 10 percent is also presented in table III. In some cases the time required for a given weight loss is estimated. These estimations were based on the weight-loss-rate trends established by other specimens with the same coating. Although a weight loss of 10 percent was selected at the beginning of the program as the failure criteria, table III shows that in most cases the time required to reach a 10-percent weight loss was not significantly greater than the time required to reach an 8-percent weight loss. The notable exception was the coating A specimens.

Coating A(G) and coating B were not applied to the sheared-edge specimens.

Broken edges.- Weight losses of as much as 2 percent in the first hour of exposure were also observed in coated specimens with the broken-edge preparation (fig. 12). Here again, most specimens "healed" and achieved some degree of stability before a sharp increase in weight-loss rate indicated coating breakdown. Some of the broken-edge specimens exhibited the same abrupt weight gain preceding failure that was noted for the sheared-edge specimens.

All three specimens with coating E which were tested in the broken-edge condition failed within 15 minutes after exposure at 2,500° F in air. There was no apparent reason for this early failure. These specimens had received the same coating procedure as the other coating E specimens, and metallographically examined broken-edge specimens revealed no insight to the poor performance of this coating on the broken-edge specimens. The fact that all three specimens exhibited a general breakdown of the coating (table IV) would indicate that the coating procedures for these specimens were at fault and not the additional edge treatment these specimens received. The information presented in table IV for the broken-edge specimens is similar to the information presented in table III for the sheared-edge specimens.

When the broken-edge specimens were examined after testing, the initial failure point was detectable on 22 of the 25 specimens tested. Initial edge failures were noted in 9 specimens (table IV). The only specimens which did not fail predominantly at the edges were those with coating E and coating F. These were also

the only coatings which received additional edge treatment by the coating supplier prior to coating.

After a 6- to 8-percent weight loss, the broken-edge specimens also required little additional time to achieve the 10-percent weight loss which was the failure criterion. The exception to this was the coating A specimens which all failed slowly.

Tumbled edge.- The tumbled-edge specimens with coating A and coating B usually exhibited little or no weight change prior to failure (fig. 13). Specimens with the other coatings generally lost some weight initially, "healed," and then exhibited only minor additional weight changes prior to the start of failure. The reversal in weight change preceding the start of failure observed in the broken- and sheared-edge specimens was also noted in most of the tumbled-edge specimens.

Thirty specimens were tested with tumbled edges and of these, 5 of the 28 failures which could be classified were edge failures (table V). The specimens with coating B were the only ones in this series of tests which failed on an edge predominately. It is interesting to point out, however, that none of these failed initially at the hole which was drilled in these specimens for suspension in the fluidized bed for coating.

Substrate damage.- The investigation reported in reference 10 indicates that visual examination of specimens was not a reliable method for detecting initial failure or determining the full extent of substrate damage after a specimen had failed. Figures 14 to 20 show photographs of tested oxidation specimens. The "a" parts of figures 14 to 20 show some typical specimens after a weight loss of at least 10 percent. Even after this large weight loss, the full extent of substrate damage is not evident until the specimen is mechanically probed. The "b" parts of figures 14 to 20 show the full extent of damage after the specimen was probed with a sharp instrument to remove all unsound material. Although all the specimens pictured revealed obvious points of failure after 10 percent or more weight loss, the results of the probing investigations clearly indicate the questionable value of visual examination as the sole method for the detection of initial coating breakdown.

Edge effects.- Comparison of the average lifetimes for the three edge conditions investigated (fig. 21) suggests that the effect of different edge conditions is quite pronounced. With the exception of the coating A and coating C specimens, the tumbled and sheared edges provided longer lifetimes than the broken edges. The superior oxidation resistance of the sheared over the broken-edge coated specimens in the continuous-exposure test (fig. 21) may be attributed to less cold-working in fabrication, rather than to the shape of the edge prior to coating. In addition to the preferential deposition rate which commonly occurs at sharp corners in chemical deposition processes (ref. 2), the higher residual stresses evidenced in the broken edges (fig. 10) may also promote a more rapid coating deposition. When cooled from the coating temperature, the increased coating thickness on the broken edges in combination with the thermal-expansion mismatch between the molybdenum substrate and the molybdenum disilicide coating would increase the severity of the radial cracks commonly found on the edges of the coated sheet. The unsupported projections of the coating (fig. 10) resulting from these radial cracks would be more prone to damage, and as a result, may reduce coating performance.

The rounded edge of the tumbled-edge specimens, in addition to the lower residual stresses inherent with the tumbling operation, resulted in an even coating thickness and less severe radial cracking (fig. 10). This uniformity of coating thickness on the edges would be expected to produce a coating which is more reliable and less prone to edge failures.

The elimination of edge failures was noted in reference 2 as one way to improve coating reliability. Eliminating the broken- and sheared-edge specimens with coating E and coating F because of the additional edge treatment they received, the percentage of edge failures for the failures which could be classified in tables III, IV, and V are as follows:

Sheared edges, percent	40.0
Broken edges, percent	53.0
Tumbled edges, percent	26.3

The combination of reduced coating life for the majority of the coatings investigated and a higher frequency of edge failures clearly indicates that the broken edge is the least desirable (in terms of coating life) of the edge preparations investigated. Although the difference in oxidation performance between the tumbled-edge and sheared-edge specimens for most of the coatings tested (fig. 21) was not significant, the lower frequency of edge failures in the tumbled-edge specimens would indicate that the tumbled edge was the most desirable edge preparation tested.

Cyclic-Exposure Oxidation Tests

The three types of cyclic tests which were performed in this study were chosen to evaluate the various coatings under representative cyclic thermal exposure and to compare the lifetimes of the various coatings with the continuous-exposure results.

The cyclic tests were performed on tumbled-edge specimens. The maximum temperature was held constant at 2,500° F and the length of exposure at temperature and the temperature-rise rates were varied.

0.1-hour cycle.- In the 0.1-hour-cycle tests the specimens were subjected to a rapid temperature-rise rate, allowed to stabilize at 2,500° F for a short period, and then subjected to a rapid cooling. As in the continuous-exposure tests, the failure criterion was a weight loss of 10 percent. The specimens were weighed after each cycle and inspected visually for signs of failure. Plots of weight change for a typical specimen of each coating tested are presented in figure 22. Because the specimens were not weighed during the cycle, all weight changes between cycles were assumed to be linear during each cycle.

Typically, the specimens with coating C, coating E, and coating F gained weight during the first few cycles, reached a maximum, and then continued to lose weight until failure. The A and A(G) coatings either gained or lost weight slowly for many cycles and then lost weight with an increasing rate until failure. The specimens with coating B and coating D usually began to lose weight after a few cycles and then continued to lose weight at an increasing rate until failure.

The intitial location of failure in each specimen in the cyclic tests was easily determined for each specimen tested because of the opportunity to observe the specimen between cycles. Table VI presents the results of these initial failure-location determinations. In every specimen tested, the initial failure and in most cases the only failure point occurred on an edge of the specimen. Table VI also presents the time required for each specimen tested to sustain weight losses of 2, 4, 6, 8, and 10 percent.

1.0-hour cycle.- Although the specimens in the 1.0-hour-cyclic tests were exposed to 2,500° F for a longer period of time than the specimens in the 0.1-hour cycle, the trends of weight change with respect to the number of cycles (fig. 23) were essentially the same. The specimens with coating C and coating E gained weight rapidly, reached a maximum, and then continued to lose weight until failure with the specimens with coating C failing more rapidly. The specimens with coating B and D did not gain weight; the coating B specimens exhibited some stability before failure, and the coating D specimens began to fail on the first cycle. The coating A, coating A(G), and coating F specimens gained weight slowly, reached a maximum, and lost weight with a gradually increasing rate. The initial locations of failure in these tests were also the edges (table VII). Only one specimen of those tested did not fail initially on an edge. The time required to sustain the various weight losses presented in table VII is based on the assumption that weight losses during each cycle were linear.

0.5-1.0-0.5—hour cycle.- The slow heating and cooling incorporated in the 0.5-1.0-0.5—hour cycle did not subject the specimens to any appreciable thermal shocking. This cycle did, however, subject the specimens to temperatures between 1,500° F and 2,500° F for approximately 0.4 hour in addition to the hour in each cycle at 2,500° F.

The plots of weight change (fig. 24) are similar in nature to the other two cyclic tests. The coating C, coating E, and coating F specimens attained their maximum weight quickly and then started to fail with the coating E and coating F specimens failing slowly. The coating B and coating D specimens exhibited no stability and began to fail on the first cycle. The weight-loss rate for coating D specimens was high and remained essentially constant to failure. The specimens with coating A and coating A(G) gained weight slowly, reached a maximum, and then failed rapidly. The coating A specimens were the only specimens tested in the 0.5-1.0-0.5—hour cyclic tests which did not consistently fail initially on an edge (table VIII). Table VIII also presents the time required for each specimen to undergo weight losses of 2, 4, 6, 8, and 10 percent. The weight losses during each cycle were again assumed to be linear.

Comparison of cyclic tests.- The average number of cycles required to produce a 10-percent weight loss for each coating evaluated in the three types of cyclic-exposure tests is compared in figure 25. With the exception of coating E and coating F specimens, the additional time at 2,500° F in the 1.0-hour test compared with the 0.1-hour test was detrimental to the number of cycles to failure. This detrimental effect is evidenced by the fact that the specimens with coating A, coating A(G), coating B, coating C, and coating D all failed in fewer 1.0-hour cycles than 0.1-hour cycles. The specimens with coating E and coating F appeared to be less affected by the additional time at the temperature of the 1.0-hour cycle than by the number of cycles. For the specimens with coating E and coating F, the

average number of cycles to failure was essentially the same for the 0.1-hour and 1.0-hour cycles.

During the 0.5-1.0-0.5—hour cycles, the specimens were exposed to temperatures between 1,500° F and 2,500° F for 0.4 hour each cycle, in addition to the 1 hour at 2,500° F. The oxidation rate of molybdenum is significant above 1,500° F and the oxidation product (MoO_3) is volatile above this temperature. In view of the fact that the average number of cycles to failure in the 1.0-hour cycles was not significantly reduced when the specimens with coating C and coating D were subjected to the 0.5-1.0-0.5—hour cycles, it would appear that the specimens with coating C or coating D were not sensitive to the additional time at temperatures from 1,500° F to 2,500° F encountered during the slow heating and cooling cycles. The specimens with coating B and coating F appeared to be sensitive to the time at temperatures below 2,500° F. Even with the pessimistic assumption that the additional 0.4 hour per cycle above 1,500° F produced the same degradation of the coating as comparable time at the test temperature (and consequently should be added to the time required to produce failure), the resulting average time to failure in the 0.5-1.0-0.5—hour cyclic tests on the specimens with coating B and coating F would be less than in the 1.0-hour cyclic tests. This low-temperature sensitivity of the coating F specimens may be indicative of "pest" type failures. When the coating E specimen average life in hours is given the benefit of this assumption, the agreement in average lifetimes between the 1.0-hour and 0.5-1.0-0.5—hour cycles is close - 20.0 to 20.4 hours. The specimens with coating A and coating A(G) were the only ones tested in which the average number of cycles to failure in the 0.5-1.0-0.5—hour cyclic test was significantly greater than the number required in the 1.0-hour cyclic tests. Although the 0.5-1.0-0.5—hour cycle reduced any damage which may have been caused by thermal shocking in the 1.0-hour cycle, it would appear that the additional time spent below 2,500° F in the 0.5-1.0-0.5—hour cycle was beneficial to the oxidation resistance of these coatings. This improvement could be due to the low-temperature formation of a boron-modified SiO_2 protective surface.

The cyclic tests provided a good opportunity to observe the initiation of failure, and as previously mentioned, visual examination was an unreliable method of detection. After each cycle the specimens were inspected, and in some cases a weight loss of 3 percent did not produce a visible defect in the coating. When a visible defect was found, the specimen was probed to reveal the full extent of substrate damage. Some typical examples of these initial defect points are presented in figures 26(a), 27(a), and 28(a). Figures 26(b), 27(b), and 28(b) present these same specimens after failure. In figure 28 the final failure appears to be only an extension of the original defect. The continued oxidation of the initial defect to produce a 10-percent weight loss was not the only mode of failure. In most of the cycled specimens, other points of failure on the edges were initiated before a 10-percent weight loss terminated the test (figs. 26 and 27). These additional edge failures indicated that the edges of the cycled specimens were marginally protected by the coating when the specimens were subjected to thermal cycling. When the test was terminated, the full extent of substrate damage was not apparent until after the specimens were probed to remove unsound material. Figures 29, 30, and 31 show typical failed specimens before and after probing.

Initial failures adjacent to the suspension hole were noted in some of the coating B specimens. This mode of failure indicated that the method of suspension in the fluidized bed interfered with the proper application of the coating in this area. Although the suspension hole in the coating B specimens resulted in an additional edge in the coating, the suppliers' procedures for hole preparation appear to be adequate and only a few specimens failed initially in the edges of the hole.

Comparison of continuous- and cyclic-exposure tests.- The ability of a coating to protect the substrate when continually exposed to a constant temperature is, for most applications of coated refractory sheet material, an unrealistic indicator of its performance under the cyclic-temperature exposures which would normally be encountered in service. The average accumulated times at 2,500° F before failure for the various coatings under the cyclic- and continuous-exposure tests are compared in figure 32. This figure clearly indicates the severe reduction in coating performance for all the coatings subjected to cyclic exposure.

Weight Changes and Failure Mechanisms

In this section an attempt will be made to explain qualitatively the weight changes which were observed during both the continuous- and cyclic-exposure tests and the mechanisms which were operative in the failure of these specimens. While various phenomena may be associated with the oxidation failures, the proposed failure mechanisms are supported by the test results.

Continuous-exposure tests.- Some of the continuously exposed specimens exhibited an initial weight loss (figs. 11, 12, and 13), which may be attributed to at least two phenomena. Part of this initial weight loss may be attributed to the oxidation of the substrate. This initial substrate oxidation occurs through cracks or fissures in the coating which result from stresses present at room temperature in the system due to the difference in the thermal expansion between the coating and the substrate. At the deposition temperature (approximately 2,000° F), the coating forms on the substrate under no stress. Below the deposition temperature, the coating would be in tension because of its higher thermal expansion (fig. 33). Conversely, above the deposition temperature, the coating would be in compression. If the tensile strength of the coating is exceeded when the composite is cooled, the coating will crack. When initially exposed to temperature, these cracks would allow the oxidation of the substrate. However, they would soon seal as the temperature of the coated specimen exceeds the deposition temperature.

Part of this initial weight loss may also be attributed to the oxidation of $MoSi_2$. The oxidation resistance of $MoSi_2$ is considered to be due to the formation of a protective layer of SiO_2 which forms when $MoSi_2$ oxidizes (ref. 11) in the following manner:

$$2MoSi_2 + 7O_2 \rightarrow 2MoO_3 + 4SiO_2$$

This reaction would result in a net weight loss. The weight-loss rate would be expected to decrease as the SiO_2 film formed and protected the $MoSi_2$ from further oxidation. The possibility of another oxidation reaction for $MoSi_2$ is suggested in reference 12. This reaction

$$5MoSi_2 + 7O_2 \rightarrow Mo_5Si_3 + 7SiO_2$$

would result in a net weight gain in the coated specimen as the protective SiO_2 film was formed.

Reference 12 further states that both of these reactions are probably taking place when the $MoSi_2$ oxidizes and that the reaction to form $Mo_5Si_3 + SiO_2$ is thermodynamically favored as the oxygen activity decreases - such would be the case as the SiO_2 film continues to grow. As the reaction to form $Mo_5Si_3 + SiO_2$ becomes predominant, the specimens would gradually gain weight. This gradual weight gain was, in fact, observed after the initial weight loss (figs. 11, 12, and 13) on some specimens and is further supported by the detection of Mo_5Si_3 near the surface of the specimens by X-ray diffraction. The detection of Mo_5Si_3 near the surface can not be reasonably explained by diffusion in view of the fact that the work presented in reference 6 indicates that $MoSi_2$ is present between the Mo_5Si_3 layer and the Mo-0.5Ti substrate.

The rapid increase in weight-loss rate, which was indicative of coating breakdown and subsequent specimen failure, was in some cases preceded by a small abrupt weight gain (fig. 13). This weight gain was observed on specimens with all three edge conditions and would indicate that oxygen penetrated the coating surface and was trapped. This trapped oxygen could then react with the remaining coating and/or the substrate. Reference 6 indicates that even after a few hours of exposure solid-state diffusion of silicon from the coating toward the substrate would have increased the molybdenum concentration in the coating resulting in the formation of the higher molybdenum silicides, Mo_5Si and Mo_3Si, at the expense of the $MoSi_2$ in the coating. This mechanism is in addition to the aforementioned oxidation reaction which also results in the formulation of Mo_5Si_3. Silicides Mo_3Si and Mo_5Si_3 are known to have less stability in an oxidizing atmosphere than $MoSi_2$ (ref. 13), and consequently the ability of any remaining coating to protect the substrate would be reduced.

Any molybdenum trioxide forming as an oxidation product would be highly volatile at the test temperature of 2,500° F (ref. 14). If the oxidation product could not escape as fast as the reaction was taking place, the buildup of pressure caused by the volatile MoO_3 would finally rupture the coating, allow a more rapid oxidation of any remaining coating and/or molybdenum substrate, and result in a rapid weight loss. This mode of failure is supported by obvious "blow holes" observed in tested specimens (figs. 14(a) and 15(a)).

If the infusion of oxygen into the coating occurred gradually and the oxidation products were not totally confined, the volatile oxidation product might only distort and bubble the coating. The distorted coating would then allow more rapid penetration of oxygen and the failure would continue at an accelerating rate but would result in a series of cracked bubbles in the coating with no violent eruptions. This type of failure would be expected to occur when there was a general breakdown of the coating which would allow the oxidation products to escape without building up sufficient pressure to erupt violently. This type of failure can be seen in figures 16(a) and 17(a) where the surface of the specimens contains

numerous bubbles and cracks in the coating. It is interesting to note that specimens which failed by numerous bubbles and breaks in the coating, showed strong α cristobalite patterns when examined by X-ray diffraction and had the milky color which is characteristic of this crystalline form of silica.

The investigation reported in reference 15 is concerned with the oxidation of SiC, which like $MoSi_2$, forms a protective layer of SiO_2 when oxidized. The oxide layer which was observed in the investigation of reference 15 was initially amorphous and then transformed into cristobalite after an incubation period which was a function of the test temperature. The oxidation of the SiC was assumed to be controlled by diffusion. A sharp increase in the oxygen-diffusion constant was noted when the amorphous SiO_2 layer transformed into cristobalite. The increase in the rate of oxygen penetration associated with the formation of cristobalite observed in the oxidation of SiC and the detection of cristobalite on the failed specimens in this study indicate that the formation of a crystalline form of silica on the surface of the coatings tested was detrimental and severely reduced the ability of the coatings to protect the substrate. This mechanism is further supported by the fact that the coating A and coating A(G) specimens were the only ones which did not typically reveal large amounts of cristobalite after failure. Furthermore, these specimens exhibited longer lifetimes, usually failed gradually, and had detectable amounts of boron in the coating which gave indications of inhibiting the formation of cristobalite and supporting the growth of an amorphous silica outer layer on the coating (ref. 9). In addition, the one coating A specimen which did fail prematurely (no. 33 table V) contained an abnormally high concentration of cristobalite on the surface of the coating.

Cyclic-exposure tests.- Cyclic exposure of the coatings tested resulted in a sharp reduction in coating performance (fig. 32) and an increase in the percentage of edge failures (tables V to VIII).

Some of the cyclically exposed specimens also exhibited net weight gains which were not observed in the continuously exposed specimens. This net weight gain (figs. 22, 23, and 24) indicates that an additional mechanism was operative when the specimens were cyclically exposed as contrasted with the continuous exposure to the test temperature. The only way $MoSi_2$ can gain weight when oxidizing is by the formation of $Mo_5Si_3 + SiO_2$, and this reaction is favored when the activity of the oxygen present at the oxidizing interface is low.

The X-ray analysis of failed coated specimens revealed that the protective outer layer typically contained a large percentage of α cristobalite. The volume change which occurs when β cristobalite transforms into α cristobalite (fig. 33) at about 570° F may result in sufficient shrinkage to relieve the compressive stresses in the oxide layer. In addition, this shrinkage may be of sufficient magnitude to crack the outer layer. Although not visually detected, evidence of this cristobalite phase change and the resultant cracking of the coating surface was observed. When removed from the furnace, faint cracking sounds were heard on some of the specimens as they cooled below about 700° F to 500° F. No cracking was heard above this temperature range, nor was the cracking heard for any length of time as the specimens cooled further. When the specimen is reheated after the oxide formation, any cracks in the oxide layer would seal below 1,000° F after the cristobalite phase change. Because the $MoSi_2$ phase of the coating is still in

tension, any gases remaining in the cracked coating or at the $MoSi_2$-SiO_2 interface would be trapped.

The activity of oxygen at the SiO_2-$MoSi_2$ interface would be low if it had been trapped on reheating, and the resealed oxide layer would provide a definite barrier to rapid oxygen penetration from the outer surface of the oxide to replenish the oxygen which reacted with the $MoSi_2$. As was pointed out in the discussion of the weight changes in the continuous-exposure oxidation tests, both of the oxidation reactions are probably taking place with the reaction to form the volatile MoO_3 initially being favored. After the formation of an oxide layer thick enough to decrease the availability of oxygen at the oxide-coating interface, the reaction to form Mo_5Si_3 and SiO_2 would be favored, and the specimen would gain weight if the substrate and/or the oxide layer were not failing. This cracking of the coating and subsequent trapping of gases would be expected to occur predominately on the edges of the specimens because of the more severe cracks which occur in these areas (fig. 10).

The initial weight gain which was noted on some of the specimens when cyclically exposed (figs. 22, 23, and 24) lends support to this mechanism. The coating B and coating D specimens did not exhibit initial weight gains - this is probably due to the fact that these specimens were failing and the effects of any weight gain due to the formation of Mo_5Si_3 were masked. The coating C, coating E, and coating F specimens characteristically gained weight initially, reached a maximum net weight gain, and then began to fail. In both coating C and coating E specimens, the as-coated surface contained significant amounts of constituents which would further reduce the oxygen activity at the $MoSi_2$-SiO_2 interface. Both the formation of Al_2O_3 when the $Mo(Si,Al)_2$ compound oxidized on the specimens with coating C and the formation of Cr_2O_3 on the specimens with coating E would reduce the availability of oxygen at the oxidizing interface. In addition, the oxidation products formed, being nonvolatile at the test temperature, would further increase the weight gains noted on the specimens with coating C and coating E. The weight gains noted on the coating F specimens occurred more slowly (figs. 22, 23, and 24). This weight gain is due primarily to the proposed mechanism because of the lack of detectable coating additives.

As was noted in the discussion of continuous-exposure failure, the formation of cristobalite is associated with a reduction of the ability of the coatings to protect the substrate.

The behavior of the specimens with coating A and coating A(G) lends further support to the hypothesis that the rapid formation of cristobalite severely reduced the ability of the coatings to protect the substrate when cyclically exposed. The specimens with coating A and coating A(G) exhibited the longest cyclic life of the coatings tested. These coatings contained detectable amounts of boron and are reported to contain additional coating additives. These coating additives appear to modify the coating and retard the formation of cristobalite.

Because of this modified oxide layer, the trapping of gas would not be expected to occur and the specimens would not gain weight, as can be observed in figures 22, 23, and 24.

Room-Temperature Tensile Tests

Room-temperature tensile properties for Mo-0.5Ti molybdenum-alloy sheet after application of various oxidation resistant coatings are presented in table IX. Room-temperature tensile properties of uncoated stress-relieved Mo-0.5Ti sheet are also given in the table for comparison purposes. Typical stress-strain curves for the uncoated sheet and for the coated specimens in both the longitudinal and transverse grain directions are presented in figure 34. The effect of the various coating procedures on the room-temperature ultimate tensile strength, 0.2-percent offset yield stress, Young's modulus, and elongation in 2 inches are shown in figure 35 as ratios of the corresponding properties of the uncoated Mo-0.5Ti sheet. All stresses in table IX and figures 34 and 35 are based on specimen areas before coating.

It can be seen in figures 35(a) and 35(b) that the coating procedures used in application of the coatings B, C, and D had the least effect on the tensile and yield stresses - reducing these stress values less than 20 percent. The procedures used in application of coating E and coating F reduced the ultimate strength approximately 30 percent and reduced the yield stress approximately 40 percent. The application of coating A and coating A(G) had the most severe effect in that it reduced the ultimate and yield stresses of the Mo-0.5Ti sheet by approximately 60 percent.

Figure 35 indicates that application of any of the coatings investigated herein had a small effect on Young's modulus. In this case the effect of reduction of modulus (based on original specimen area) due to reduced substrate thickness will tend to be counteracted by the increase in modulus due to recrystallization and a small load-carrying capacity in the coating.

As shown in figure 35, the application of coating E and coating F had the least effect on room-temperature elongation of the Mo-0.5Ti sheet - reducing this value less than 20 percent. The application of coating B, coating C, and coating D reduced elongation 20 percent in the longitudinal direction and 50 to 60 percent in the transverse direction. The application of coating A(G) had the most severe effect - reducing the room-temperature elongation of the Mo-0.5Ti sheet by approximately 70 percent.

The characteristics of some heats of Mo-0.5Ti molybdenum-alloy sheet are such that complete recrystallization of cold-rolled and stress-relieved sheet will result in a decrease in both room-temperature tensile strength and elongation (ref. 16). Partial recrystallization of stress-relieved Mo-0.5Ti sheet may result in a reduction of room-temperature strength with a small increase in elongation. In view of these characteristics, the results presented in figure 35 and the hardness and recrystallization data presented in reference 6 on the as-coated material indicate that the properties of the Mo-0.5Ti sheet were substantially affected only by the magnitudes of the temperatures and times used in the coating application and not by the presence of the coating.

CONCLUSIONS

An investigation has been made to evaluate the oxidation protection afforded Mo-0.5Ti molybdenum-alloy sheet by several silicide-based coatings. Emphasis is placed on a better understanding of edge failures and the reduction of coating life when thermally cycled. The following conclusions are made from the data presented herein:

1. Cyclic exposure at 2,500° F in air severely reduces the ability of most of the coatings tested to protect the Mo-0.5Ti sheet.

2. Abrasive tumbling of the thin-gage specimens resulted in smoothly rounded edges prior to coating and improved the oxidation performance for most of the coatings tested.

3. Cyclically exposed coated specimens failed on the edges more frequently than specimens which were continuously exposed to the test temperature.

4. The experimental data substantiate the failure mechanisms proposed for both the continuous- and cyclic-exposure oxidation tests.

5. Coatings which formed amorphous outer layers when exposed to high-temperature air were the most protective.

6. The formation of cristobalite on the surface of the coatings was strongly associated with coating failures.

7. Visual examination of coated specimens as the sole method for the detection of initial failure or extent of substrate damage was an unreliable method.

8. Application of the protective coatings investigated generally reduced the mechanical properties of the Mo-0.5Ti substrate because of the time-temperature history required for coating application.

9. Continuous weighing of coated specimens during high-temperature exposure was helpful in describing the mechanisms which may be operative in coating breakdown.

Langley Research Center,
National Aeronautics and Space Administration,
Langley Station, Hampton, Va., August 29, 1963.

[REFER TO DMIC No. 56906 FOR ADDITIONAL INFORMATION ON THESE COATINGS, ESPECIALLY DIFFUSION DATA.]

END

APPENDIX A

EQUIPMENT AND PROCEDURES FOR CONSTANT-TEMPERATURE OXIDATION TESTS

The constant-temperature oxidation tests in this investigation were conducted in the vertical tube furnace shown in figure 36. The heated chamber of this furnace consisted of two vertical alumina tubes of $2\frac{1}{2}$-inches inside diameter. The tubes were heated by silicon carbide heating elements supported horizontally in the furnace. Ten elements were arranged in five pairs with the elements of each pair in a vertical plane on opposite sides of the tubes. The pairs were arranged on a vertical axis so that a uniformly heated length approximately 4 inches long was available at the midlength of each alumina tube. The temperature in the tubes was proportionally controlled by a saturable reactor power supply which used a platinum/platinum 10-percent rhodium thermocouple as a sensor. The thermocouple was immersed in a protection tube which was placed between the two vertical alumina tubes at their midheight. A thermocouple was inserted into the test chamber to determine the proper set point on the furnace controller so that the heated zone would be at the 2,500° F test temperature. These calibration tests indicated that the temperature variations in the testing zone and the temperature fluctuations with time did not exceed ±0.5 percent of the test temperature (2,500° F). The bottom ends of the tubes were closed, and cover plates were used on the tops of the tubes during a test. A 3/4-inch hole was cut in the cover plates to allow freedom for the suspension wire and the escape of any volatile oxidation products. No attempt was made to control the mass flow or quality of the atmosphere in the test chambers. Any airflow was produced by convection currents which were set up in the tube and the small leakage of laboratory air around the bottom tube closures.

The coated oxidation specimens were supported in a zircon boat which was suspended in the furnace on a platinum wire. No reactions were observed between any of the test specimens and the zircon boat at 2,500° F.

The oxidation specimens were expected to survive many hours of exposure to the test temperature, and continuous monitoring of the test by an operator was not practical. For this reason the weight of the specimens was continually recorded by an automatic balance. In addition to indicating failure, it was hoped that the continuous record of specimen weight with time would provide additional insight into the mechanisms of protection and failure of the various coatings under investigation. The balances - one for each tube - were supported on a separate frame above the oxidation furnace (fig. 36). A closeup view of the balance assembly is shown in figure 37(a). The balance consisted of a long beam which was supported by a hardened steel knife edge on a heat-treated 17-4 PH stainless-steel fulcrum. A hook was provided at one end of the beam to support the specimen suspension wire. Rigidly attached to the other end of the beam was the core plug of a linearly variable differential transformer (L.V.D.T.) and a magnet. Below the magnet was a solenoid. The coil and the L.V.D.T. were rigidly attached to a vertical rod. The operation of the balance depended on the fact that the attractive force produced on the magnet by the solenoid is linearly dependent on the current in the coil so long as the magnet does not change its location in the field of solenoid.

When the beam was in the balanced condition, the L.V.D.T. was in the null condition. When the specimen changed weight, the beam was displaced and the L.V.D.T. generated a signal which reflected the magnitude and direction of the weight change. This signal was amplified and used as the control voltage for a servomotor. The servomotor drove a 10-turn potentiometer, which changed the current flowing in the solenoid and restored the beam to a balanced condition. The change in current in the solenoid was a linear function of the weight change and was continuously recorded. A schematic diagram of the circuit is shown in figure 37(b). A paddle attached below the fulcrum point was immersed in silicone oil to damp the beam. In the configuration shown, the automatic balance was capable of detecting a weight change of 2 milligrams which represented a change in weight of approximately 0.05 percent for the specimens tested. The maximum weight change which could be detected without taring was 500 milligrams. The stability of the balance assembly, specimen boat, and the suspension wire was recorded for periods up to 400 hours. The maximum recorded weight change for the system, including the effects of the test temperature on the zircon boat and platinum suspension wire, never exceeded 20 milligrams and in most cases did not exceed 10 milligrams.

The specimen to be tested was inserted into the zircon boat which was at room temperature. The boat and specimen were then manually lowered into one of the vertical tubes which had been previously heated to the test temperature. The suspension wire was attached to the hook on the balance. The balance was then switched to the automatic weighing mode and any necessary tare weights were added to the balance. The specimen insertion and taring normally required only about 2 minutes, and the complete system was stabilized in approximately 3 minutes. The insertion or removal of a specimen in one tube did not disturb the specimen in the other tube.

APPENDIX B

EQUIPMENT AND PROCEDURES FOR CYCLIC-EXPOSURE OXIDATION TESTS

The furnace and associated equipment used to subject the coated specimens to a variety of exposure times for the cyclic-exposure oxidation tests are shown in figure 38.

This box furnace has a uniformly heated chamber 6 inches high, 12 inches long and 12 inches wide. It is heated by 16 molybdenum-disilicide hairpin heating elements which are suspended from the roof of the furnace with 8 elements on each side of the heated zone. The temperature in the chamber is proportionally controlled by a saturable reactor power supply which uses a platinum/platinum 10-percent rhodium thermocouple as the temperature sensor. The thermocouple is immersed in a protection tube which is suspended from the roof of the furnace and terminates in the uniformly heated zone.

For the 0.1-hour and 1.0-hour rapid-heating cycles, the specimen was supported in a zircon boat which was placed on a foamed silica hearth and inserted into the test chamber through a small opening in an auxiliary furnace door. The zircon boat was constructed to allow more than one specimen to be tested at a time. Calibration tests were run to determine the proper controller set point to achieve a specimen temperature of 2,500° F. Two-color optical-pyrometer observation on coated specimens indicated that approximately 95 percent of the test temperature was achieved on the specimens 30 seconds after insertion. The time at temperature for both the 0.1-hour and the 1.0-hour cycles started when the specimen was inserted into furnace and ended upon removal. The specimen normally cooled to below 1,500° F in 20 seconds.

For the slow heating and cooling cycles, an electromechanical specimen inserter was constructed which controlled the rate of specimen insertion into and removal from the furnace. A zircon boat was attached to the end of an alumina rod which in turn was attached to a servocontrolled rack and pinion drive. The output of a platinum/platinum 13-percent rhodium thermocouple, attached to the alumina rod and in close proximity to the specimen, was compared with the output of a curve-following function generator. The resultant error signal was then used as the control signal for the servomotor which drove the inserter track in the proper direction to bring the specimen to the programed temperature. At the beginning of a test, the inserter was withdrawn about 6 inches from the furnace door and the specimen was placed in the zircon boat. The function generator was then activated and the specimen was advanced into the furnace. The function generator was programed to control linearly the temperature-rise rate of the specimen. The specimen reached the test temperature in 30 minutes, was exposed to the test temperature for 1 hour, and was then removed from the furnace. The cooling rate was also linearly controlled by the function generator and it required 30 minutes to cool from 2,500° F to room temperature. Calibration tests indicated that the actual specimen temperature did not vary more than 2 percent from the desired specimen temperature throughout the complete cycle.

APPENDIX C

FURNACE COMPARISON TESTS

The continuous-exposure and cyclic-exposure oxidation tests were conducted in different furnaces (appendixes A and B), and in order to evaluate the results of these tests, it was necessary to compare the oxidizing conditions which existed in each furnace. The comparison specimens were fabricated from commercially pure molybdenum 0.040-inch sheet approximately 1.0 inch long by 0.6 inch wide. The specimens were weighed and measured and then exposed for 5 minutes at 2,500° F. Specimens were oxidized in each tube of the vertical tube furnace and in the box furnace.

The weights of the specimens before and after testing, original area (including edges), and the exposure time were used to compute oxidation rate in $mg/cm^2/hr$. The results of these comparison tests are as follows:

Facility	Average linear weight loss, $mg/cm^2/hr$
Front vertical tube	1,420
Rear vertical tube	1,615
Box furnace	2,260

As mentioned in appendix A no attempt had been made to seal the ends of the vertical tubes completely and the difference in average linear weight losses was not considered significant enough to affect appreciably the test results for the coated specimen. The difference in weight-loss rate in the vertical tube and box furnaces was appreciable.

There was no appreciable airflow in either furnace, and because of this, the oxidation rate of the bare molybdenum tabs was probably controlled by diffusion as a result of the blanketing effects of the volatile oxidation product (MoO_3). Although the oxidation rate of bare molybdenum is reported to increase with increasing mass flow (refs. 13, 16, and 17), no references could be found which contained similar information on coated molybdenum. In order to investigate the effect of the more severe oxidizing conditons in the box furnace, specimens coated with three different coatings were selected for continuous-exposure oxidation tests in the box furnace. A balance assembly similar to those used with the automatic balances, was modified to operate in the box furnace. The tumbled-edge coating E, broken-edge coating C, and broken-edge coating D specimens were selected for continuous-exposure testing at 2,500° F in the box furnace. The results of these tests are presented in tables IV and V and the specimens are noted by the letter b before the specimen number. Typical weight-change plots are shown in figure 39 for these specimens.

Although the specimens continuously exposed in the box furnace did not typically exhibit the large initial weight loss that was noted on the specimens exposed

in the vertical tube furnace (fig. 13), the general shape of weight-loss plots was the same. The more rapid "healing" of the coatings in the box furnace did not seem to improve the oxidation life of coating D and coating E specimens which were continuously exposed in the box furnace (tables IV and V). The specimens with coating C exhibited longer times to failure in more severe oxidizing conditions in the box furnace which may be due to the presence of $Mo(Si,Al)_2$ that was detected on the as-coated surface in significant amounts.

REFERENCES

1. Krier, C. A.: Coatings for the Protection of Refractory Metals From Oxidation. DMIC Rep. No. 162, Battelle Memorial Inst., Nov. 24, 1961.

2. Blumenthal, Herman, and Rothman, Neil: Development of a Powder and/or Gas Cementation Process for Coating Molybdenum Alloys for High Temperature Protection. Final Report (Contract No. AF 33(616)-7383), Wright Air Dev. Div., U.S. Air Force, July 1961.

3. Chao, P. J., Payne, B. S., Jr., and Priest, D. K.: Development of a Cementation Coating Process for High-Temperature Protection of Molybdenum. ASD Tech. Rep. 61-241, U.S. Air Force, June 1961.

4. Campbell, J. E., Goodwin, H. B., et al.: Introduction to Metals for Elevated-Temperature Use. DMIC Rep. No. 160, Battelle Memorial Inst., Oct. 27, 1961.

5. Gibeaut, W. A., and Maykuth, D. J.: Summary of the Sixth Meeting of the Refractory Composites Working Group. DMIC Rep. No. 175, Battelle Memorial Inst., Sept. 24, 1962.

6. Stein, Bland A., and Lisagor, W. Barry: Diffusion Studies of Several Oxidation Resistant Coatings on Mo-0.5Ti Molybdenum Alloy at 2,500° F. NASA TN D-2039, 1964.

7. Cullity, B. D.: Elements of X-Ray Diffraction. Addison-Wesley Pub. Co., Inc., 1959.

8. Chu, Gordon P. K.: Notes on Siliconizing of Molybdenum. The Sixth Meeting of the Refractory Composites Working Group. ASD-TDR-63-610, U.S. Air Force, 1963.

9. Kingery, W. D.: Introduction to Ceramics. John Wiley & Sons, Inc., c.1960.

10. Mathauser, Eldon E., Stein, Bland A., and Rummler, Donald R.: Investigation of Problems Associated With the Use of Alloyed Molybdenum Sheet in Structures at Elevated Temperatures. NASA TN D-447, 1960.

11. Nicholas, M. G., Pranatis, A. L., et al.: The Analysis of the Basic Factors Involved in the Protection of Tungsten Against Oxidation. ASD-TDR-62-205, U.S. Air Force, June 1962.

12. Searcy, Alan W.: Predicting the Thermodynamic Stabilities and Oxidation Resistances of Silicide Cermets. Jour. American Ceramic Soc., vol. 40, no. 12, Dec. 1957, pp. 431-435.

13. Berkowitz, Joan B.: Kinetics of Oxidation in the Mo-Si System. Part 1. ASD-TDR-62-203, U.S. Air Force, May 1962.

14. Anthony, Frank M., and Pearl, Harry A.: Investigation of Feasibility of Utilizing Available Heat Resistant Materials for Hypersonic Leading Edge Applications. Vol. III - Screening Test Results and Selection of Materials. WADC Tech. Rep. 59-744, U.S. Air Force, July 1960.

15. Jorgensen, Paul J., Wadsworth, Milton E., and Cutler, Ivan B.: Oxidation of Silicon Carbide. Jour. American Ceramic Soc., vol. 42, no. 12, Dec. 1959, pp. 613-616.

16. Houck, J. A.: Physical and Mechanical Properties of Commercial Molybdenum-Base Alloys. DMIC Rep. 140, Battelle Memorial Inst., Nov. 30, 1960.

17. Wilks, C.: Oxidation of Molybdenum. Space Studies ER 11244-4, The Martin Co., June 1960.

18. Modisette, Jerry L., and Schryer, David R.: An Investigation of the Role of Gaseous Diffusion in the Oxidation of a Metal Forming a Volatile Oxide. NASA TN D-222, 1960.

19. Goldsmith, Alexander, Waterman, Thomas E., and Hirschhorn, Harry J.: Handbook of Thermophysical Properties of Solid Materials. Vol. IV – Cermets, Intermetallics, Polymerics, and Composites, The Macmillian Co., 1961.

TABLE I.- PERTINENT INFORMATION FOR SEVERAL OXIDATION-RESISTANT COATINGS FOR Mo-0.5Ti MOLYBDENUM ALLOY

Coating designation	Method of application	Elements in pack or bed	Source of information
A	2-cycle pack	Si, B, Cr, Cb, Al, C	Ref. 1, p. 111
A(G)	2-cycle pack cementation; 1 hour at 2800° F	Si, B, Cr, Cb, Al, C	Ref. 1, p. 111
B	Fluidized bed	Si	Ref. 1, p. 95
C	2-cycle pack cementation	Si, Cr, Al	Ref. 1, p. 113
D	2-cycle pack cementation	Si, Cr	Ref. 2
E	2-cycle pack cementation	Si, Cr	Ref. 3
F	1-cycle pack cementation	Si, Cb	Ref. 3

TABLE II.- PHYSICAL MEASUREMENTS OF SPECIMENS

Coating	Average coating thickness,[1] in.	Substrate thickness,[1] in.		Weight change, percent
		Before coating	After coating	
A(G)	0.0017	0.0122	0.0092	2.20
A	.0017	.0122	.0099	2.20
B	.0015	.0108	.0081	-3.81
C	.0014	.0120	.0106	3.43
D	.0012	.0121	.0109	4.40
E	.0023	.0118	.0091	13.67
F	.0019	.0116	.0097	7.92

[1]Based on cross section of tumbled-edge specimen.

[2]Preglassed 1 hour at 2,800° F by the coating supplier.

TABLE III.- TIME REQUIRED TO SUSTAIN VARIOUS WEIGHT LOSSES FOR SHEARED-EDGE COATED MOLYBDENUM ALLOY OXIDATION SPECIMENS CONTINUOUSLY EXPOSED AT 2,500° F IN AIR

Coating	Specimen	Time required to sustain weight loss, hr, of -					Weight loss at end of test, percent	Total exposure, hr	Mode of failure
		2 percent	4 percent	6 percent	8 percent	10 percent			
A	33	119.5	127.0	143.5	160.0	178.5	12.76	229.9	Edge
	38	122.0	166.5	223.5	-----	>261.8	7.56	261.8	Edge
	40	58.0	165.0	175.0	180.0	184.5	14.82	192.2	General
Average		99.8	152.8	180.7	-----	>208.3	-----	-----	
C	3	2.0	2.6	3.3	4.0	4.7	13.53	5.7	Edge
	4	12.9	13.0	13.1	13.2	13.2	17.47	13.6	General
	5	11.9	12.6	12.8	12.9	13.0	20.96	13.2	General
	6	9.0	10.0	10.4	10.8	11.2	12.57	11.5	Edge
	7	22.5	23.0	23.2	23.4	23.5	16.05	23.7	General
	8	9.8	10.5	10.9	11.1	11.2	15.32	11.8	Edge
	9	22.0	22.4	23.0	23.8	[a]23.8	9.56	23.4	Edge
	10	.5	23.1	23.8	23.9	24.0	12.86	24.2	General
Average		11.3	14.6	15.1	15.4	15.7	-----	-----	
D	41	21.3	21.6	21.9	22.2	22.5	11.88	22.8	General
	42	.6	21.0	21.0	21.1	21.2	14.88	21.9	General
	43	.2	.6	1.7	24.3	24.6	12.27	25.2	General
	45	.7	19.8	20.5	20.7	20.8	14.44	21.2	-------
	46	.8	20.2	20.4	20.5	20.8	12.97	21.8	-------
	48	.4	1.0	3.8	21.5	21.6	19.00	22.2	General
	49	.1	.9	1.9	3.4	[a]4.8	8.50	4.1	-------
Average		3.4	12.2	13.0	19.1	19.5	-----	-----	
E	11	4.2	5.8	6.5	7.1	7.4	14.47	7.6	General
	15	.8	3.1	4.1	5.0	5.9	14.02	7.4	General
	18	.5	.6	8.1	8.4	8.8	15.33	11.0	Edge
Average		1.8	3.2	6.2	6.8	7.4	-----	-----	
F	21	35.1	36.5	37.6	38.5	39.3	10.18	39.6	General
	22	29.7	32.9	34.6	35.6	36.2	13.86	37.2	General
	23	36.0	38.7	39.4	40.1	41.6	12.47	42.6	General
Average		33.6	36.0	37.2	38.1	39.0	-----	-----	

[a]Time required for 10-percent weight loss estimated.

TABLE IV.- TIME REQUIRED TO SUSTAIN VARIOUS WEIGHT LOSSES FOR BROKEN-EDGE COATED MOLYBDENUM ALLOY OXIDATION SPECIMENS CONTINUOUSLY EXPOSED AT 2,500° F IN AIR

Coating	Specimen	Time required to sustain weight loss, hr, of -					Weight loss at end of test, percent	Total exposure, hr	Mode of failure
		2 percent	4 percent	6 percent	8 percent	10 percent			
A(G)	33	80.5	106.0	123.0	131.0	[a]169.5	9.27	167.2	Edge
	34	37.0	56.0	64.0	68.5	77.5	14.45	116.3	Edge
	40	31.0	54.5	65.5	84.0	113.5	10.89	119.6	Edge
Average		49.5	72.2	83.8	94.5	120.2	-----	-----	
A	35	99.0	200.0	212.0	215.5	218.5	17.61	226.3	General
	37	96.5	222.0	-----	-----	>264.1	4.68	264.1	Edge
	38	55.0	98.0	150.0	171.5	192.0	14.77	209.5	-------
Average		83.5	173.3	-----	-----	>224.9	-----	-----	
B	51	10.6	15.2	17.2	18.7	19.6	13.51	20.7	Edge
	52	8.9	16.9	21.3	25.3	27.3	16.72	30.7	General
	60	2.9	5.2	7.4	9.2	10.6	17.67	14.0	Edge
Average		7.5	12.4	15.3	17.7	19.2	-----	-----	
C	1	8.0	9.6	10.5	10.8	11.0	15.94	11.4	General
	2	3.5	3.8	4.0	4.3	4.6	13.95	5.0	Edge
	[b]6	16.2	16.4	16.8	17.7	18.4	28.36	20.0	Edge
	[b]9	15.9	16.3	16.7	17.1	17.5	24.19	20.0	-------
Average		10.9	11.5	12.0	12.5	12.9	-----	-----	
D	43	16.2	16.4	16.5	16.6	16.6	10.65	16.6	General
	45	5.7	17.4	17.6	17.8	18.2	14.46	19.6	General
	49	.5	1.3	1.7	21.0	21.2	15.90	21.5	Edge
	[b]42	14.2	14.6	14.8	15.0	15.2	21.92	16.4	General
	[b]44	11.4	11.6	12.0	12.3	12.7	30.83	16.7	General
	[b]50	13.9	14.2	14.6	15.1	15.6	11.14	15.8	General
Average		10.3	12.6	12.9	16.3	16.6	-----	-----	
E	15	(c)	(c)	0.2	0.2	0.2	13.03	0.3	General
	18	(c)	(c)	.1	.2	.2	15.07	.2	General
	19	(c)	(c)	(c)	(c)	.1	11.60	.1	General
Average		----	-----	-----	0.2	0.2	-----	-----	
F	24	1.4	20.3	21.7	22.4	23.3	11.89	24.1	General
	27	.6	22.6	24.1	25.5	27.2	18.43	30.0	-------
	28	20.8	21.3	21.8	22.2	22.7	11.85	23.4	General
Average		7.6	21.4	22.5	23.4	24.4	-----	-----	

[a]Time required for 10-percent weight loss estimated.
[b]Tested in box furnace.
[c]Precise value not determined because of rapidity of failure.

TABLE V.- TIME REQUIRED TO SUSTAIN VARIOUS WEIGHT LOSSES FOR TUMBLED-EDGE COATED MOLYBDENUM ALLOY OXIDATION SPECIMENS CONTINUOUSLY EXPOSED AT 2,500° F IN AIR

Coating	Specimen	Time required to sustain weight loss, hr, of -					Weight loss at end of test, percent	Total exposure, hr	Mode of failure
		2 percent	4 percent	6 percent	8 percent	10 percent			
A(G)	2	1.0	68.5	172.0	197.0	266.0	11.92	335.8	Edge
	3	247.0	357.0	560.0	840.0	[a]1,000.0	9.61	976.2	General
	19	8.2	94.7	112.9	120.8	127.6	15.22	160.8	General
Average		85.4	173.4	281.6	385.9	464.5	-----	-----	
A	1	52.6	73.6	90.2	110.2	125.5	11.58	138.2	General
	8	280.5	317.0	320.5	323.9	[a]328.0	9.72	327.7	Edge
	13	.2	.6	37.5	55.0	64.7	12.62	71.2	General
	29	3.8	6.0	7.8	10.0	12.9	15.56	23.0	General
	33	-----	.1	.2	.3	.4	11.41	.4	Edge
	36	99.5	117.3	129.7	137.8	146.6	17.35	160.4	General
Average		72.8	85.8	97.6	106.2	113.0	-----	-----	
B	267	25.2	27.8	29.0	[a]29.8	[a]30.4	7.50	29.9	Edge
	268	8.2	[a]30.3	[a]32.3	[a]33.6	[a]34.6	3.74	30.0	General
	281	13.3	15.7	17.5	18.6	19.6	15.00	21.6	Edge
Average		15.6	24.6	26.3	27.3	28.2	-----	-----	
C	109	23.1	23.6	[a]24.0	[a]24.4	[a]24.8	5.32	23.8	General
	134	2.3	2.8	3.4	3.8	4.3	19.21	6.6	General
	136	4.1	6.8	10.2	11.4	11.8	18.74	12.6	General
	139	.8	8.6	9.2	9.4	9.6	16.80	9.2	General
Average		7.6	10.4	11.7	12.2	12.6	-----	-----	
D	67	3.6	22.7	23.6	25.3	27.0	15.05	42.3	General
	72	18.0	18.2	18.4	18.4	18.5	12.40	18.4	General
	77	6.3	19.6	19.9	20.2	20.3	11.32	20.3	General
Average		9.3	20.2	20.6	21.3	21.9	-----	-----	
E	180	71.9	72.1	72.2	72.3	72.3	12.64	72.3	General
	189	62.6	65.0	65.6	66.0	66.3	16.22	66.4	General
	193	1.5	68.9	69.8	69.9	70.0	10.20	70.1	-------
	169	63.8	64.4	64.8	66.7	68.5	11.50	69.7	General
	170	57.5	58.2	58.6	58.8	59.0	11.41	59.2	General
	[b]160	60.2	60.4	60.5	60.6	60.6	28.47	68.2	General
	[b]173	62.8	63.6	64.3	65.1	65.9	23.65	70.8	General
	[b]196	36.8	37.3	37.7	38.0	38.1	29.40	65.6	General
Average		52.1	61.2	61.7	62.2	62.6	-----	-----	
F	212	0.1	0.3	17.9	40.8	42.4	15.00	44.9	-------
	230	32.4	[a]34.4	[a]45.8	[a]37.2	[a]38.2	10.00	94.7	General
	241	.8	28.9	31.0	32.7	34.0	20.04	39.1	General
Average		11.1	21.2	28.2	36.9	38.2	-----	-----	

[a]Time required for 10-percent weight loss estimated.
[b]Tested in box furnace.

TABLE VI.- TIME REQUIRED TO SUSTAIN VARIOUS WEIGHT LOSSES FOR TUMBLED-EDGE COATED MOLYBDENUM ALLOY SPECIMENS EXPOSED TO 0.1-HOUR CYCLES IN AIR AT 2,500° F

Coating	Specimen	Time required to sustain weight loss, hr, of -					Weight loss at end of test, percent	Total exposure, hr	Mode of failure
		2 percent	4 percent	6 percent	8 percent	10 percent			
A(G)	21	12.6	12.8	12.8	12.9	[a]12.9	9.97	13.0	Edge
	25	10.1	10.3	10.5	10.6	10.8	11.79	10.7	Edge
	27	1.0	1.1	1.2	1.3	1.5	10.14	1.5	Edge
Average		7.9	8.1	8.2	8.3	8.4	-----	----	
A	22	18.3	18.5	18.8	19.0	19.0	12.56	19.0	Edge
	26	2.0	2.3	2.5	2.7	3.0	13.45	2.9	Edge
	28	9.0	9.3	9.5	9.7	9.9	10.74	9.8	Edge
Average		9.8	10.0	10.3	10.5	10.6	-----	----	
B	285	0.8	1.0	1.0	1.2	1.2	12.67	1.3	Edge
	302	.6	.7	.7	.8	.9	12.89	1.1	Edge
	303	.2	.3	.5	.5	.5	12.76	.6	Edge
Average		0.5	0.7	0.7	0.8	0.9	-----	----	
C	102	2.7	3.0	3.0	3.0	3.1	10.06	3.2	Edge
	132	.5	.7	.8	.9	.9	17.70	.9	Edge
	133	.5	.5	.5	.6	.6	17.25	.6	Edge
Average		1.2	1.4	1.4	1.5	1.5	-----	----	
D	61	0.4	0.5	0.6	0.6	0.7	14.58	0.8	Edge
	62	.2	.2	.2	.3	.3	10.27	.3	Edge
	90	1.2	1.5	1.6	1.6	1.6	12.86	1.7	Edge
Average		0.6	0.7	0.8	0.8	0.9	-----	----	
E	157	3.2	3.6	4.0	4.1	4.2	12.75	4.4	Edge
	176	.8	.8	.9	1.0	1.0	17.39	1.1	Edge
	177	.5	.6	.7	.7	.7	13.02	.7	Edge
Average		1.5	1.7	1.9	1.9	2.0	-----	----	
F	223	0.9	1.0	1.1	1.1	1.2	10.81	1.3	Edge
	224	.5	.5	.6	.6	1.3	10.27	1.3	Edge
	243	5.5	5.6	5.7	5.9	[a]6.0	8.90	6.0	Edge
Average		2.3	2.4	2.5	2.5	2.8	-----	----	

[a]Time required for 10-percent weight loss estimated.

TABLE VII.- TIME REQUIRED TO SUSTAIN VARIOUS WEIGHT LOSSES FOR TUMBLED-EDGE COATED MOLYBDENUM ALLOY SPECIMENS EXPOSED TO 1.0-HOUR CYCLES IN AIR AT 2,500° F

Coating	Specimen	Time required to sustain weight loss, hr, of -					Weight loss at end of test, percent	Total exposure, hr	Mode of failure
		2 percent	4 percent	6 percent	8 percent	10 percent			
A(G)	15	27.2	27.6	28.0	28.4	28.6	14.65	29.0	Edge
	31	34.2	34.5	34.8	35.3	36.0	19.65	36.0	Edge
	43	27.2	27.4	27.5	27.7	28.0	11.62	28.0	Edge
Average		29.5	29.8	30.1	30.5	30.9	-----	----	
A	16	12.4	13.0	13.4	13.8	14.0	14.47	15.0	Edge
	30	38.9	39.2	39.5	39.8	40.0	17.62	41.0	Edge
	42	9.4	9.8	10.1	10.3	10.5	15.35	11.0	Edge
Average		20.2	20.7	21.0	21.3	21.5	-----	----	
B	278	6.5	7.2	7.6	8.0	8.1	18.98	9.0	Edge
	292	4.6	5.0	5.1	5.2	5.3	18.59	6.0	Edge
	309	5.0	5.4	5.8	6.1	6.3	32.64	7.0	Edge
Average		5.4	5.9	6.2	6.4	6.6	-----	----	
C	104	5.5	5.9	6.1	6.3	6.5	23.09	7.0	Edge
	137	1.5	1.8	2.0	2.2	2.4	18.94	3.0	Edge
	145	1.5	1.5	1.7	1.9	2.1	20.08	3.0	Edge
Average		2.8	3.1	3.3	3.5	3.7	-----	----	
D	52	1.2	2.6	3.1	3.3	3.5	14.57	4.0	Edge
	70	.2	.3	.4	.6	.7	13.62	1.0	Edge
	96	.8	1.5	2.0	2.2	2.3	40.55	3.0	Edge
Average		0.7	1.5	1.8	2.0	2.2	-----	----	
E	154	19.5	21.0	21.4	21.7	22.2	23.59	23.0	Edge
	179	18.5	20.0	20.4	20.8	21.3	37.11	23.0	Edge
	199	15.2	15.7	16.1	16.4	16.6	12.10	17.0	Edge
Average		17.7	18.9	19.3	19.6	20.0	-----	----	
F	201	1.4	1.8	2.0	2.2	2.4	12.69	3.0	Edge
	225	22.6	24.0	24.2	24.3	24.5	12.07	25.0	General
	244	52.3	53.0	53.0	53.2	53.4	18.81	54.0	Edge
Average		25.4	26.6	26.4	26.6	26.8	-----	----	

TABLE VIII.- TIME REQUIRED TO SUSTAIN VARIOUS WEIGHT LOSSES FOR TUMBLED-EDGE COATED MOLYBDENUM ALLOY SPECIMENS EXPOSED TO 0.5-1.0-0.5—HOUR CYCLES IN AIR AT 2,500° F

Coating	Specimen	Time required to sustain weight loss, hr, of -					Weight loss at end of test, percent	Total exposure, hr	Mode of failure
		2 percent	4 percent	6 percent	8 percent	10 percent			
A(G)	14	116.5	124.9	7.0	128.0	128.8	11.03	130.0	Edge
	32	44.3	44.8	45.0	45.1	45.7	14.79	46.0	Edge
	44	25.0	25.2	26.0	26.0	26.1	72.00	28.0	Edge
Average		61.9	65.0	66.0	66.4	66.7	-----	-----	
A	17	55.0	59.0	59.6	60.0	60.0	19.96	61.0	General
	37	43.0	45.0	45.4	45.8	46.0	22.13	47.0	General
	41	35.0	35.2	35.4	35.5	35.6	11.61	36.0	General
Average		44.3	46.4	46.8	47.1	47.2	-----	-----	
B	277	4.5	5.0	5.0	5.1	5.2	20.19	6.0	Edge
	291	3.1	3.6	4.0	4.1	4.3	27.97	5.0	Edge
	308	2.6	3.0	3.2	3.3	3.5	17.44	4.0	Edge
Average		3.4	3.9	4.1	4.2	4.3	-----	-----	
C	106	4.8	5.1	5.3	5.6	5.8	10.62	6.0	Edge
	138	1.9	2.1	2.2	2.4	2.6	15.37	3.0	Edge
	144	1.9	2.0	2.2	2.4	2.6	15.33	3.0	Edge
Average		2.9	3.1	3.2	3.5	3.7	-----	-----	
D	54	1.6	3.0	3.2	3.4	3.6	14.73	4.0	Edge
	71	1.2	1.7	2.0	2.1	2.2	36.78	3.0	Edge
	97	3.0	4.0	4.1	4.1	4.2	43.70	5.0	Edge
Average		1.9	2.9	3.1	3.2	3.3	-----	-----	
E	153	17.0	19.2	20.2	21.0	21.2	15.96	22.0	Edge
	178	1.0	1.3	1.5	1.8	2.0	10.12	2.0	Edge
	198	16.7	18.2	18.5	18.9	19.1	47.68	20.0	Edge
Average		11.6	12.9	13.4	13.9	14.1	-----	-----	
F	202	6.3	7.0	7.4	7.6	8.0	10.10	8.0	Edge
	226	2.3	2.5	2.8	3.1	3.4	15.32	4.0	Edge
	242	6.3	6.7	7.1	7.3	7.5	13.27	8.0	Edge
Average		5.0	5.4	5.8	6.0	6.3	-----	-----	

TABLE IX.- RESULTS OF ROOM-TEMPERATURE TENSILE TESTS OF COATED Mo-0.5Ti MOLYBDENUM ALLOY SHEET[a]

Coating	Specimen (b)	σ_{tu}, ksi	σ_{ty}, ksi	E, psi	El, percent
A(G)	1L	51.4	41.0	36.4×10^6	2
	2L	76.3	45.2	37.4	5
	3L	54.0	40.0	39.0	2
	4T	43.9	39.2	38.0	2
	5T	47.2	39.9	33.3	2
	6T	54.8	42.0	44.2	2
B	7L	113.9	99.0	48.0×10^6	8
	8L	116.4	98.1	48.2	8
	9T	105.7	103.6	43.8	1
	10T	117.8	103.8	45.2	4
	11T	121.4	108.2	37.9	5
C	12L	121.0	101.4	39.5×10^6	6
	13L	118.7	98.9	39.3	9
	14L	118.5	99.7	42.8	8
	15T	133.2	118.2	42.4	3
	16T	131.0	114.5	41.3	4
D	17L	121.2	96.0	46.3×10^6	10
	18L	118.0	96.0	44.2	5
	19L	120.9	100.8	40.8	8
	20T	126.2	110.3	45.0	4
	21T	124.0	107.6	45.5	4
E	22L	96.8	71.7	44.5×10^6	9
	23L	95.4	70.2	44.0	8
	24T	105.3	82.9	41.8	7
	25T	98.8	76.5	42.3	7
F	26L	97.4	65.7	42.5×10^6	8
	27L	96.8	69.6	41.7	8
	28T	93.2	64.1	44.6	8
	29T	92.3	64.6	42.4	8
Uncoated	30L	134.5	109.0	45.0×10^6	11
	31L	133.2	110.0	43.9	12
	32L	132.4	110.4	42.1	9
	33L	133.6	109.8	44.7	10
	34T	138.7	125.8	44.6	8
	35T	141.0	123.9	46.8	8
	36T	142.1	128.4	44.2	8

[a] Nominal strain rate: 0.005 per minute to yield; 0.050 per minute to failure. (All stresses based on specimen areas before coating.)

[b] L and T indicate longitudinal and transverse grain directions.

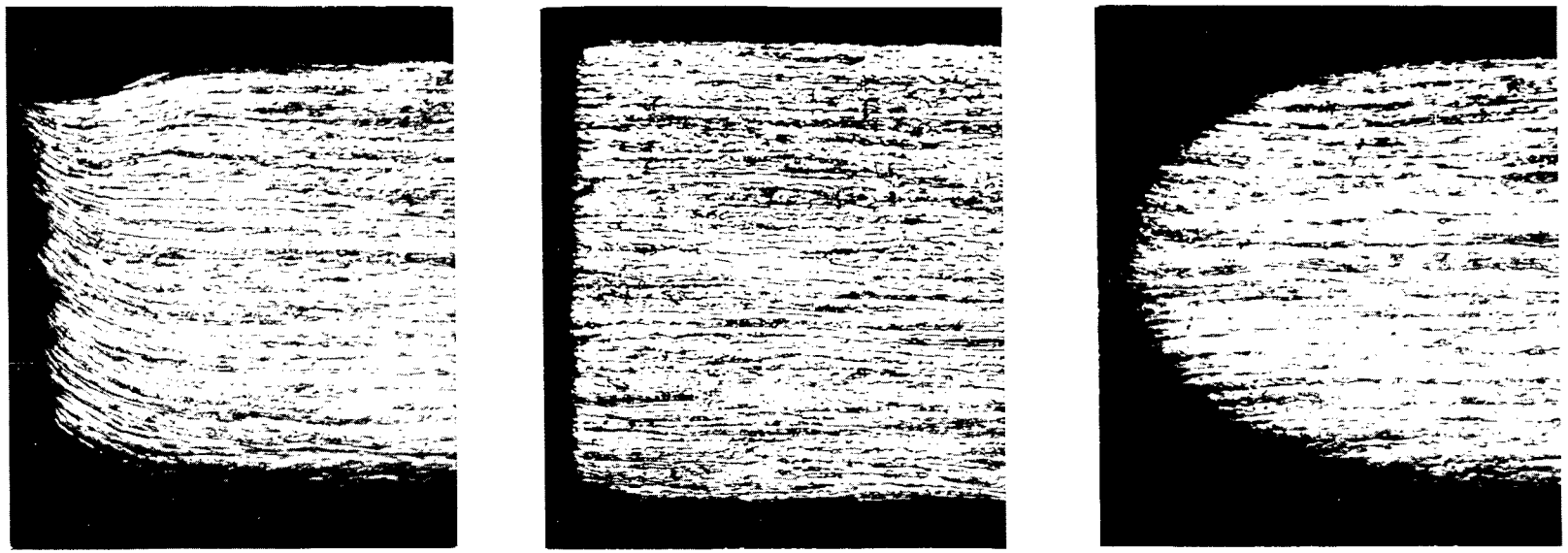

(a) Sheared edge. (b) Broken edge. (c) Tumbled edge.

L-63-4788.1

Figure 1.- Cross-sectional view of typical edges on 0.012-inch molybdenum-alloy sheet oxidation specimens before coating. Approximately X250.

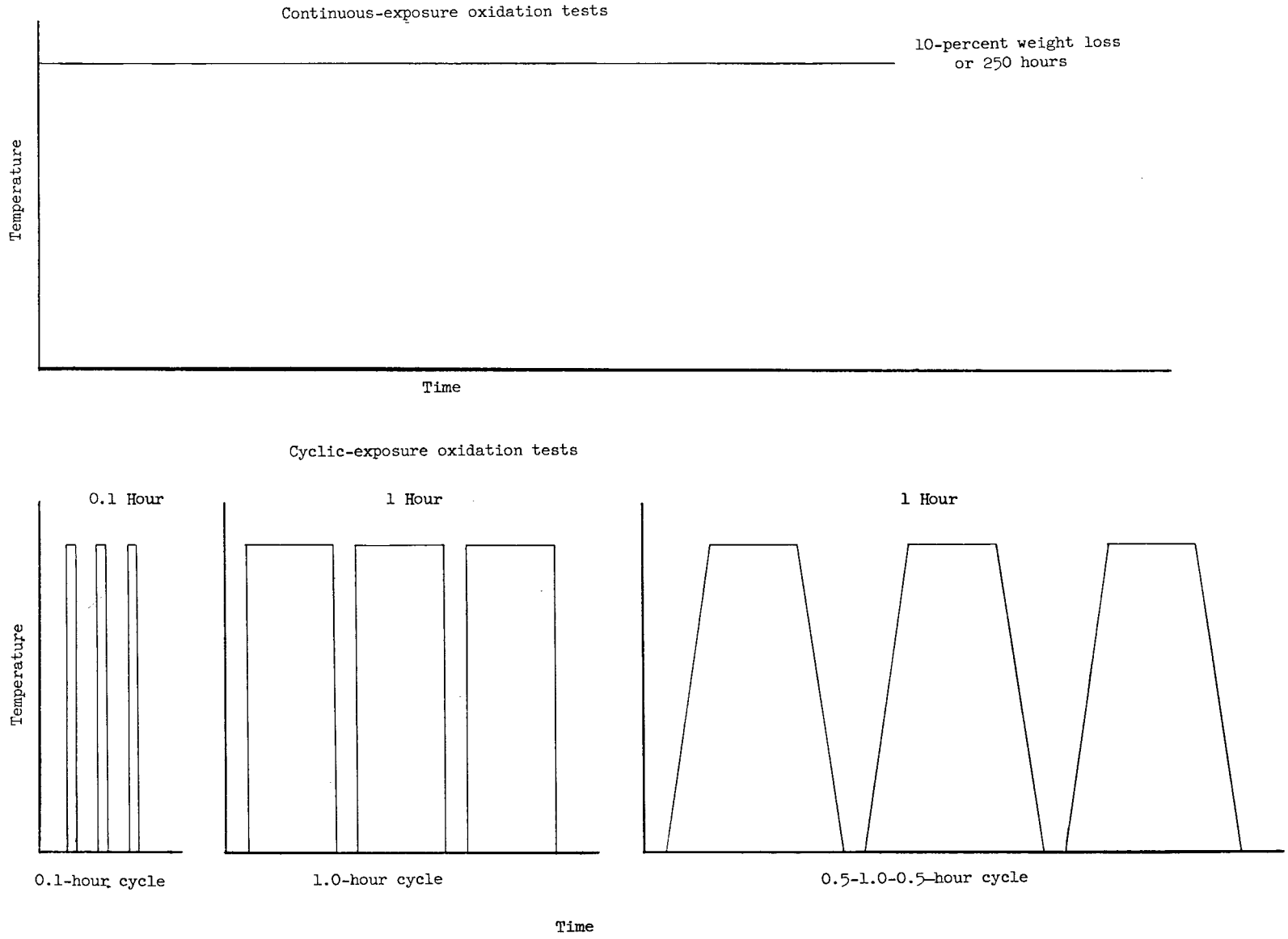

Figure 2.- Time-temperature histories for continuous- and cyclic-exposure oxidation tests at 2,500° F in air.

(a) As-coated appearance. X2.

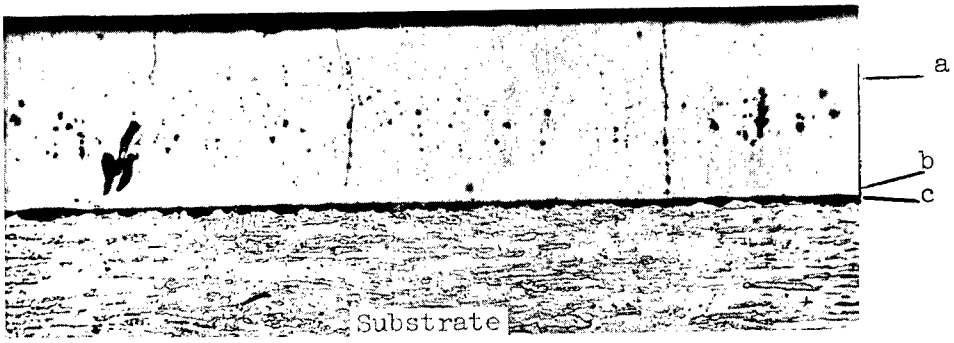

(b) Cross section, bright field illumination. X500.

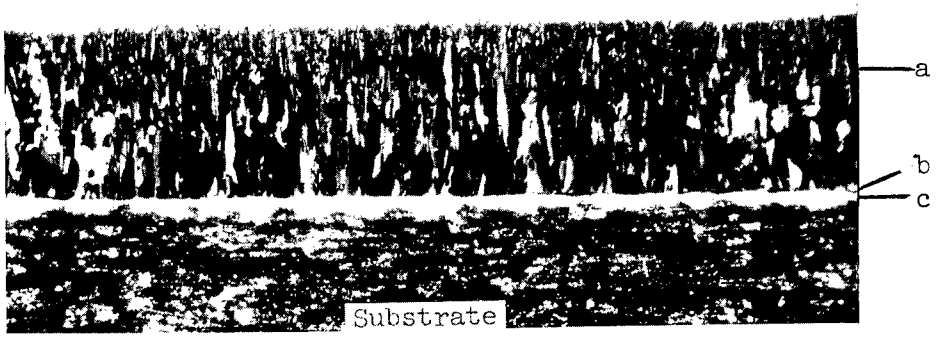

(c) Cross section, polarized light. X500.

L-63-4789

Figure 3.- As-coated coating A unglassed sheared-edge oxidation specimen.

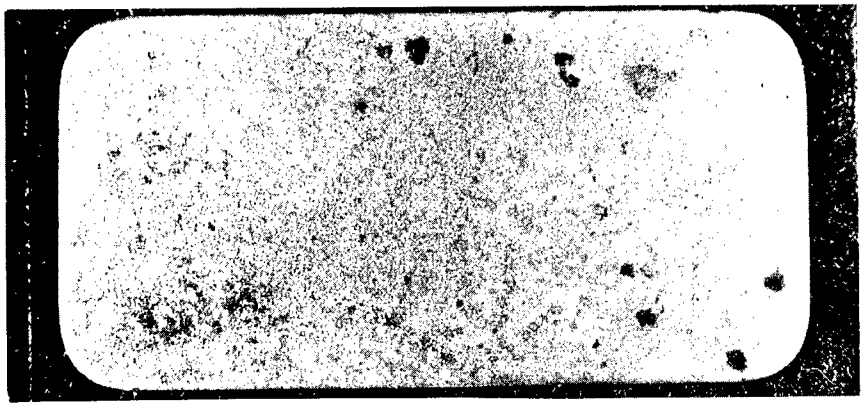

(a) As-coated appearance. X2.

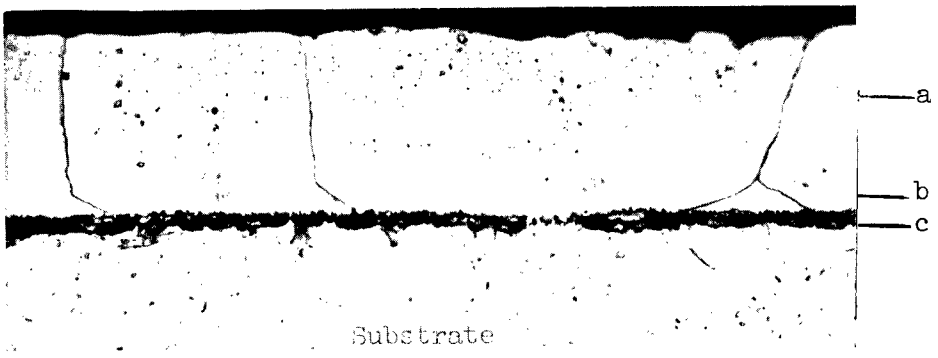

(b) Cross section, bright field illumination. X500.

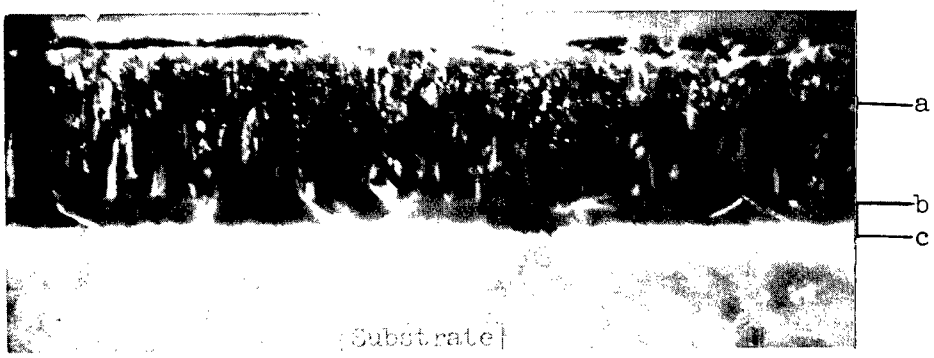

(c) Cross section, polarized light. X500.

L-63-4790

Figure 4.- As-coated coating A(G) tumbled-edge oxidation specimen.

(a) As-coated appearance. X2.

(b) Cross section, bright field illumination. X500.

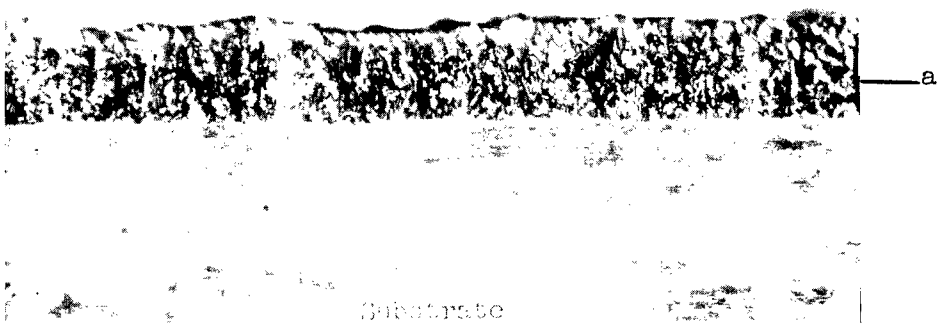

(c) Cross section, polarized light. X500.

L-63-4791

Figure 5.- As-coated coating B broken-edge oxidation specimen.

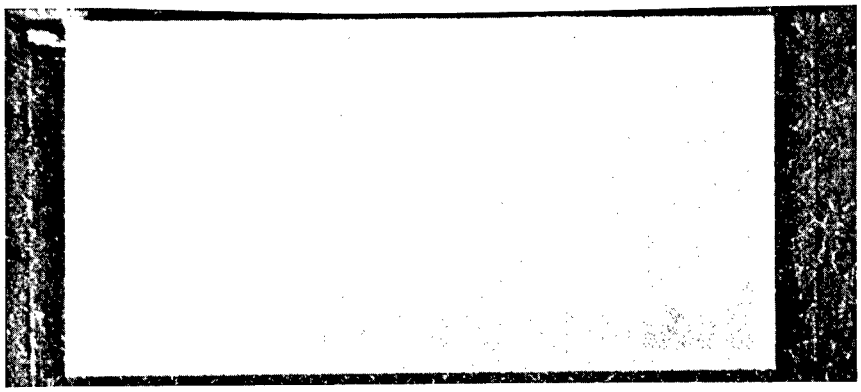

(a) As-coated appearance. X2.

(b) Cross section, bright field illumination. X500.

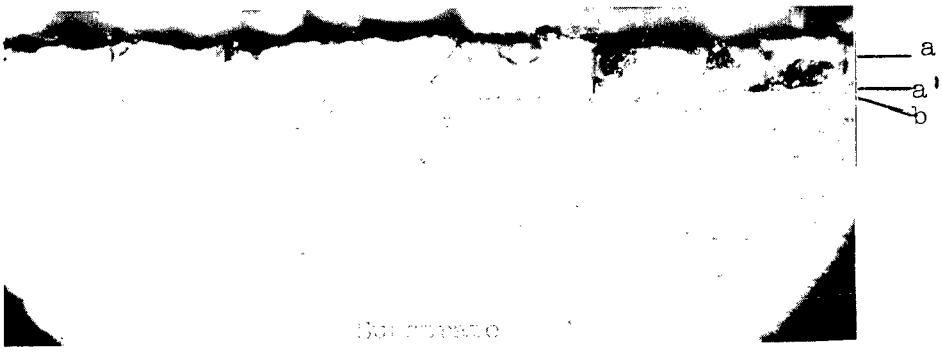

(c) Cross section, polarized light. X500.

L-63-4792

Figure 6.- As-coated coating C broken-edge oxidation specimen.

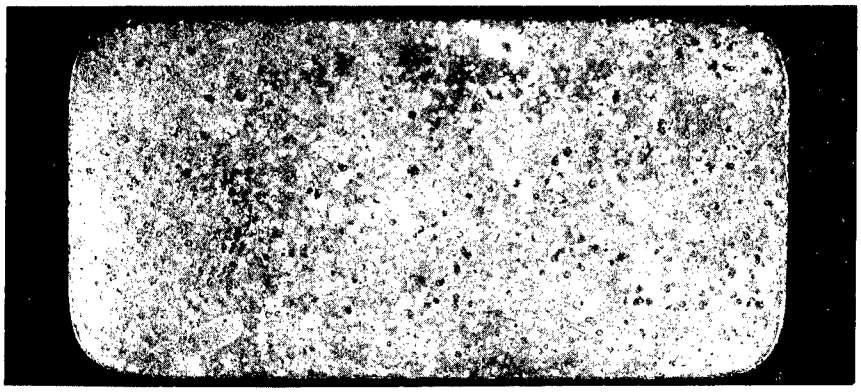

(a) As-coated appearance. X2.

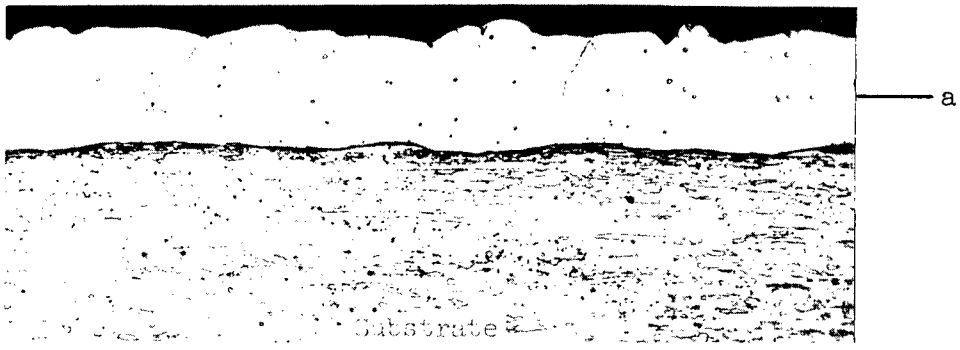

(b) Cross section, bright field illumination. X500.

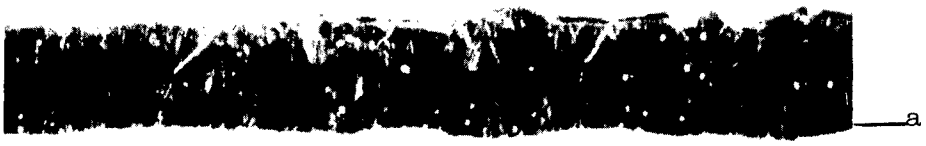

(c) Cross section, polarized light. X500.

L-63-4793

Figure 7.- As-coated coating D tumbled-edge oxidation specimen.

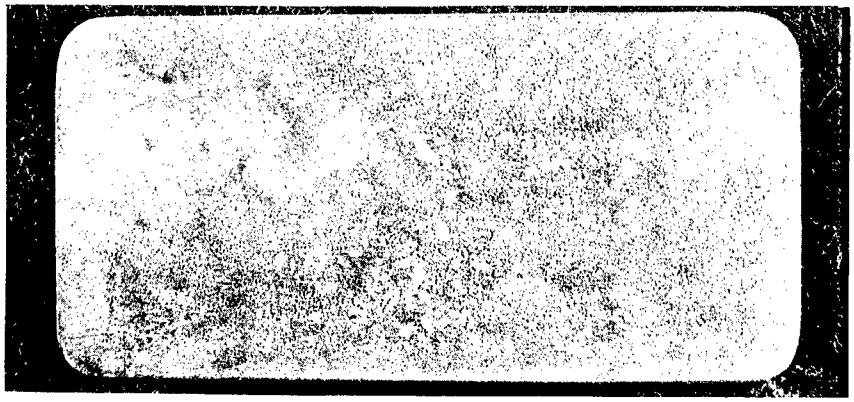

(a) As-coated appearance. X2.

(b) Cross section, bright field illumination. X500.

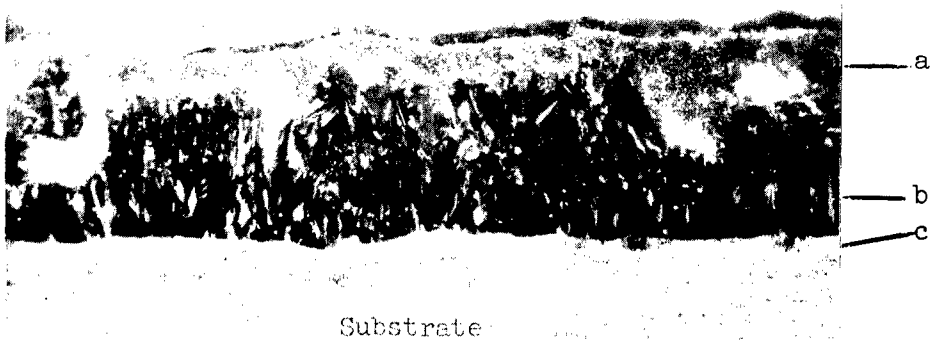

(c) Cross section, polarized light. X500.

L-63-4794

Figure 8.- As-coated coating E broken-edge oxidation specimen.

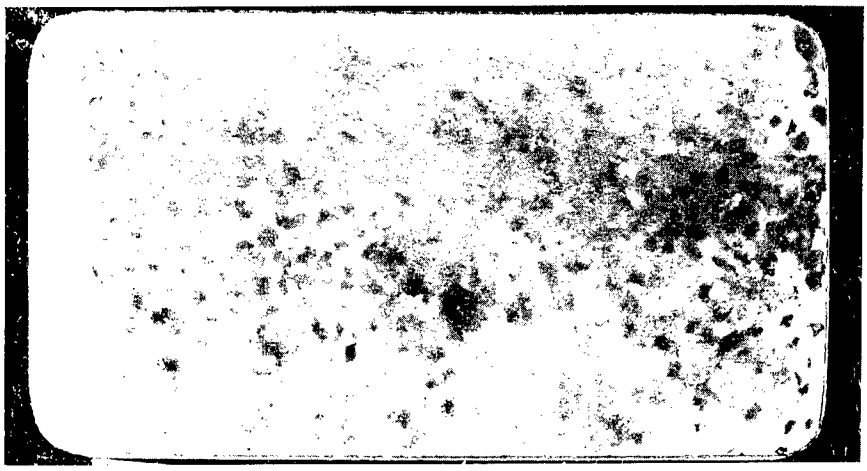

(a) As-coated appearance. X2.

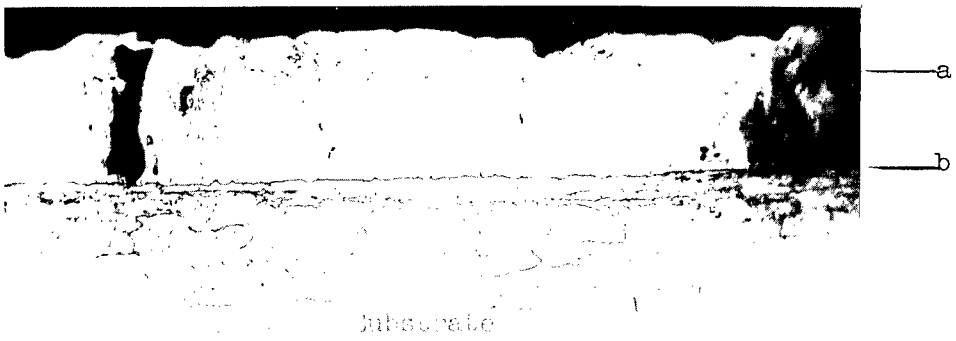

(b) Cross section, bright field illumination. X500.

(c) Cross section, polarized light. X500.

L-63-4795

Figure 9.- As-coated coating F sheared-edge oxidation specimen.

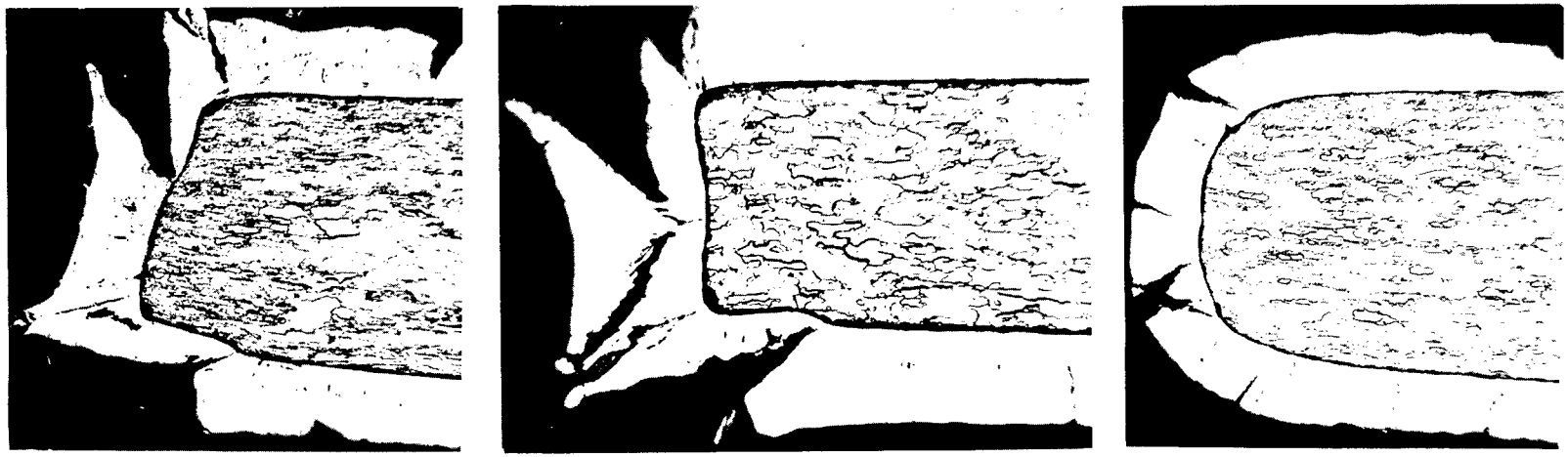

(a) Sheared edge. (b) Broken edge. (c) Tumbled edge.

L-63-4796

Figure 10.- Appearance of a typical coating after application on 0.012-inch Mo and -0.5Ti sheet specimens with three edge conditions. Approximately X150.

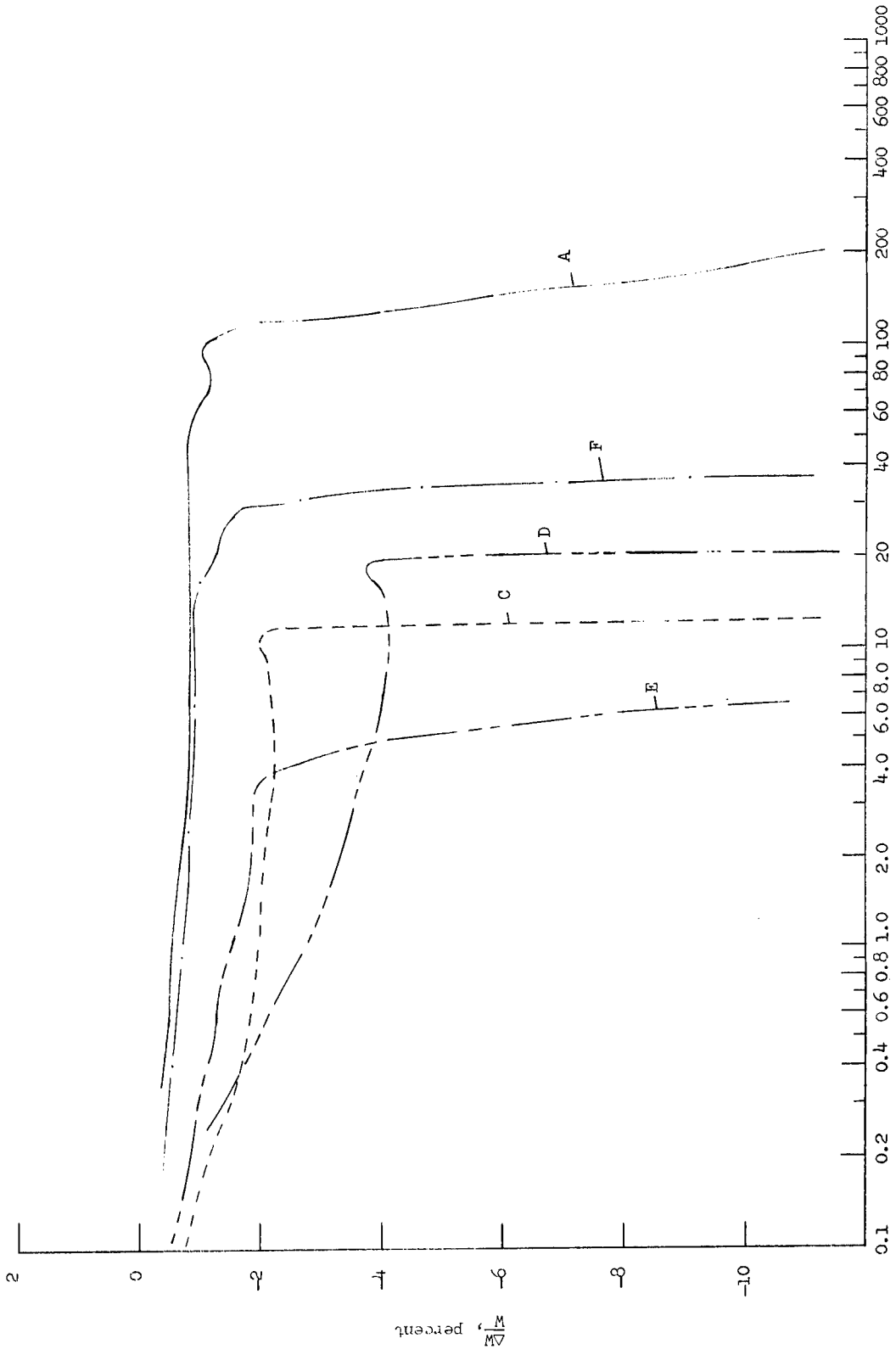

Figure 11.- Typical weight change for continuous exposure at 2,500° F for coated Mo-0.5Ti with sheared edges.

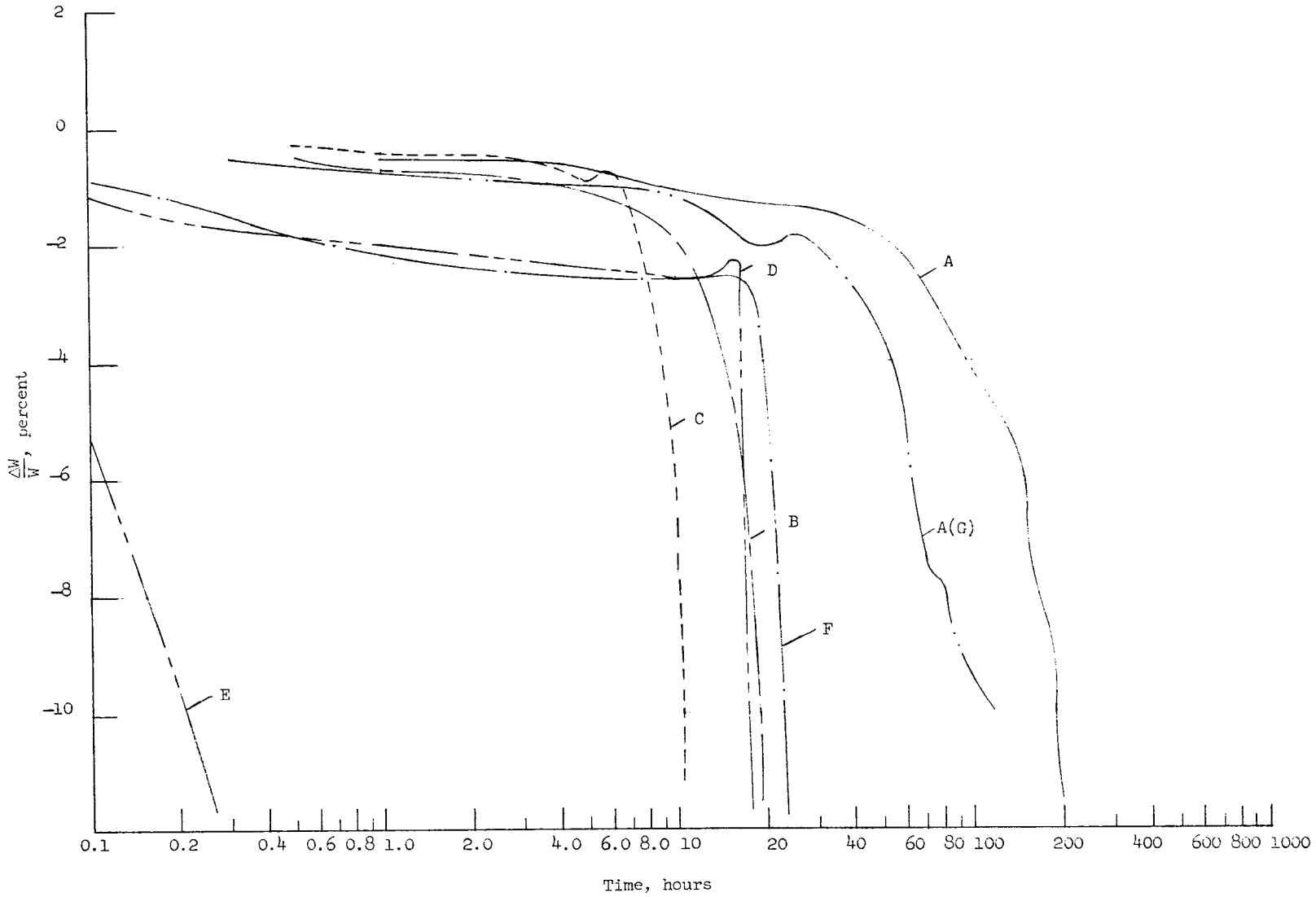

Figure 12.- Typical weight change for continuous exposure at 2,500° F for coated Mo-0.5Ti with broken edges.

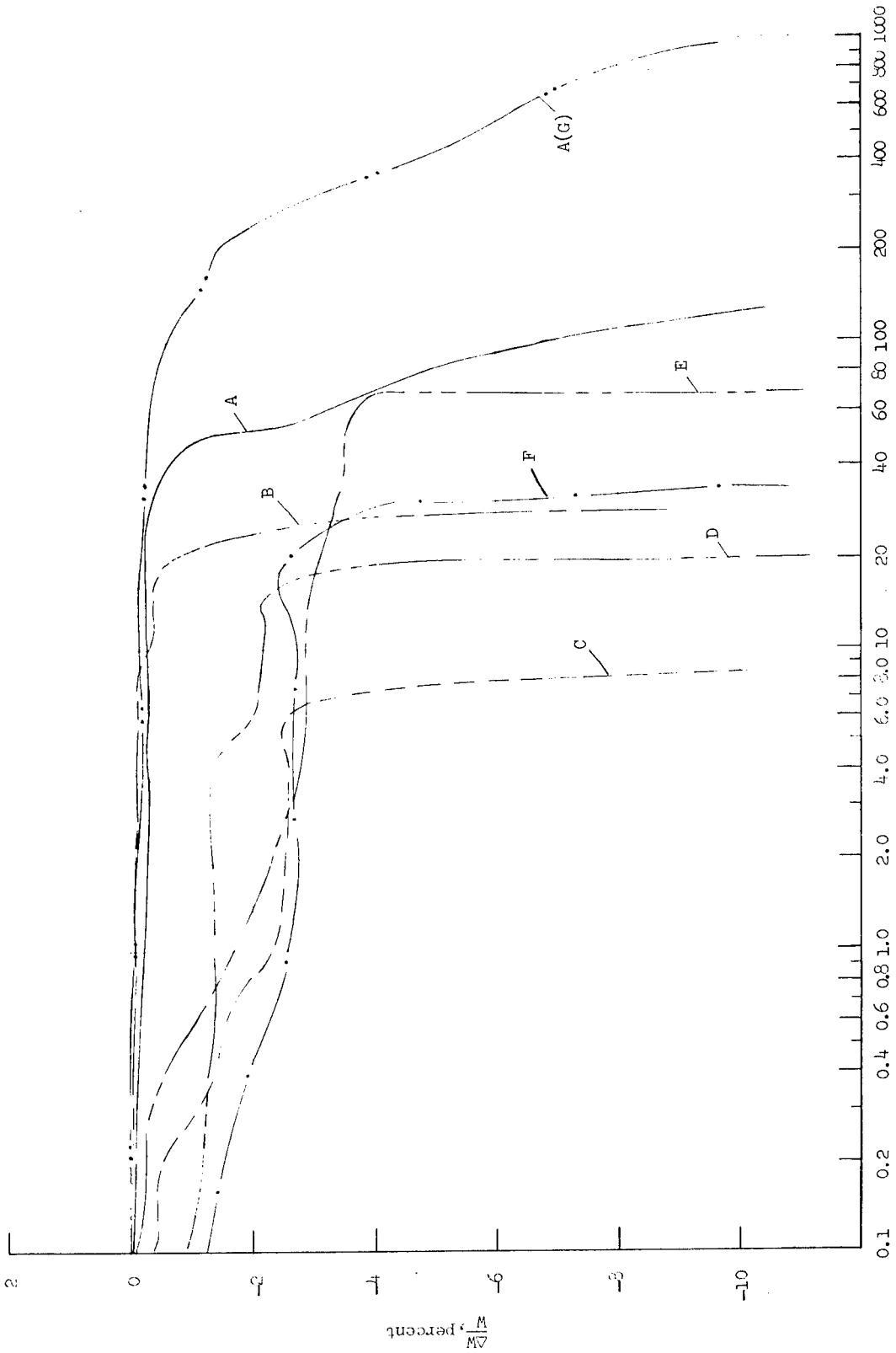

Figure 13.- Typical weight change for continuous exposure at 2,500° F for coated Mo-0.5Ti with tumbled edges.

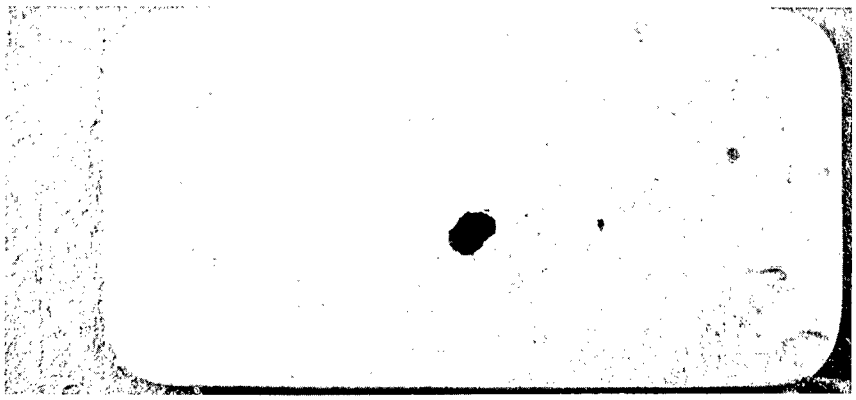

(a) Before probing.

(b) After probing.

L-63-4797

Figure 14.- Coating A(G) tumbled-edge oxidation specimen after 976.2 hours of continuous exposure at 2,500° F in air.

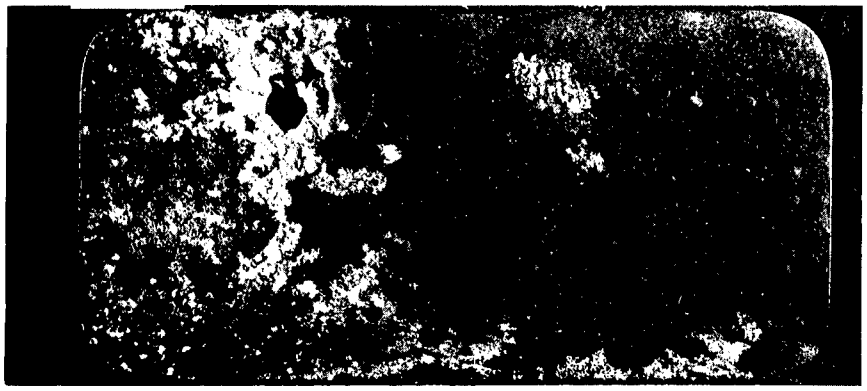

(a) Before probing.

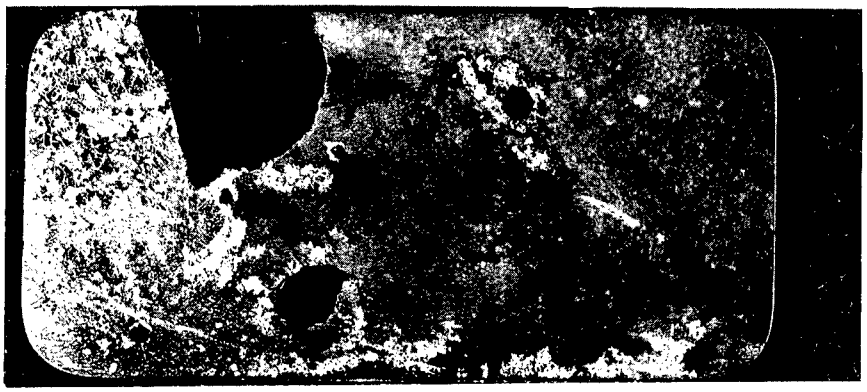

(b) After probing.

L-63-4798

Figure 15.- Coating A tumbled-edge oxidation specimen after 160.4 hours of continuous exposure at 2,500° F in air.

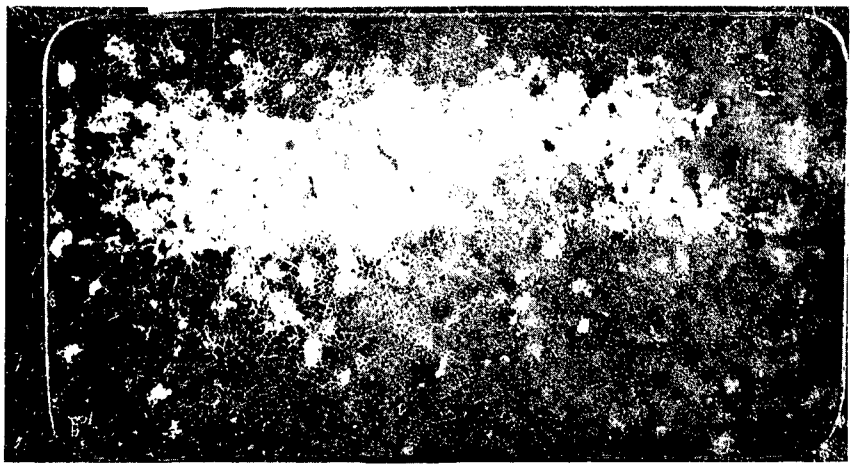

(a) Before probing.

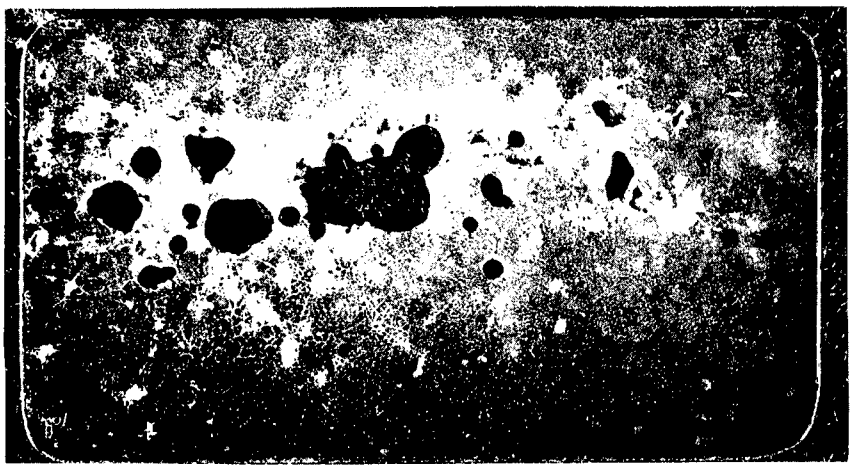

(b) After probing.

L-63-4799

Figure 16.- Coating F sheared-edge oxidation specimen after 42.6 hours of continuous exposure at 2,500° F in air.

(a) Before probing.

(b) After probing.

L-63-4800

Figure 17.- Coating D tumbled-edge oxidation specimen after 18.4 hours of continuous exposure at 2,500° F in air.

(a) Before probing.

(b) After probing.

L-63-7501

Figure 18.- Coating E broken-edge oxidation specimen after 0.1 hour of continuous exposure at 2,500° F in air.

(a) Before probing.

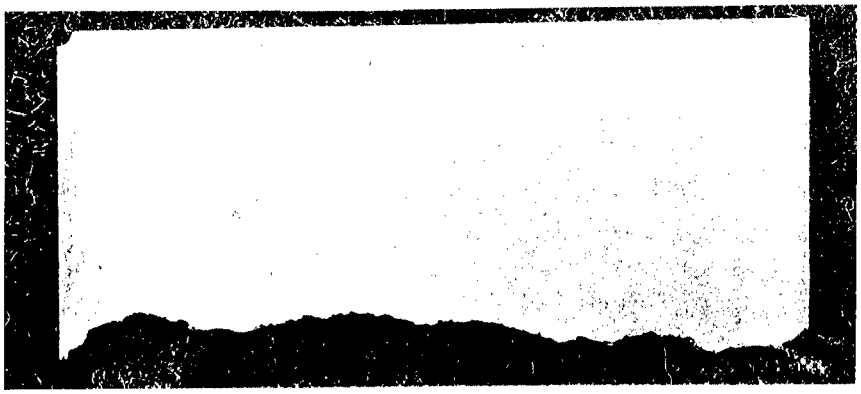

(b) After probing.

L-63-7502

Figure 19.- Coating C broken-edge oxidation specimen after 5.0 hours of continuous exposure at 2,500° F in air.

(a) Before probing.

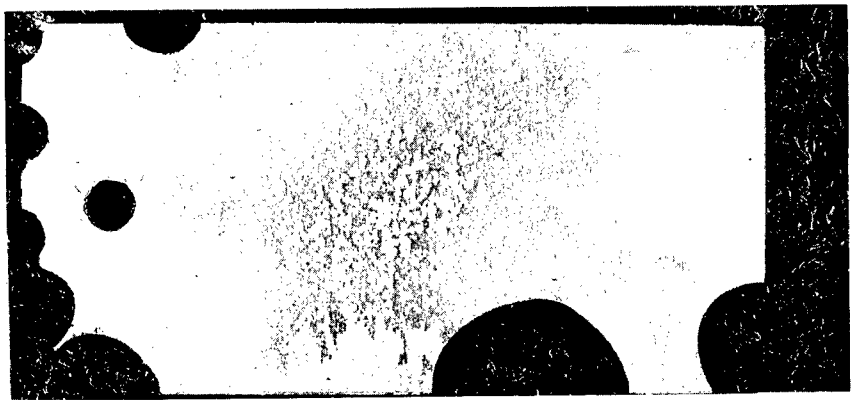

(b) After probing.

L-63-7503

Figure 20.- Coating B broken-edge oxidation specimen after 20.7 hours of continuous exposure at 2,500° F in air.

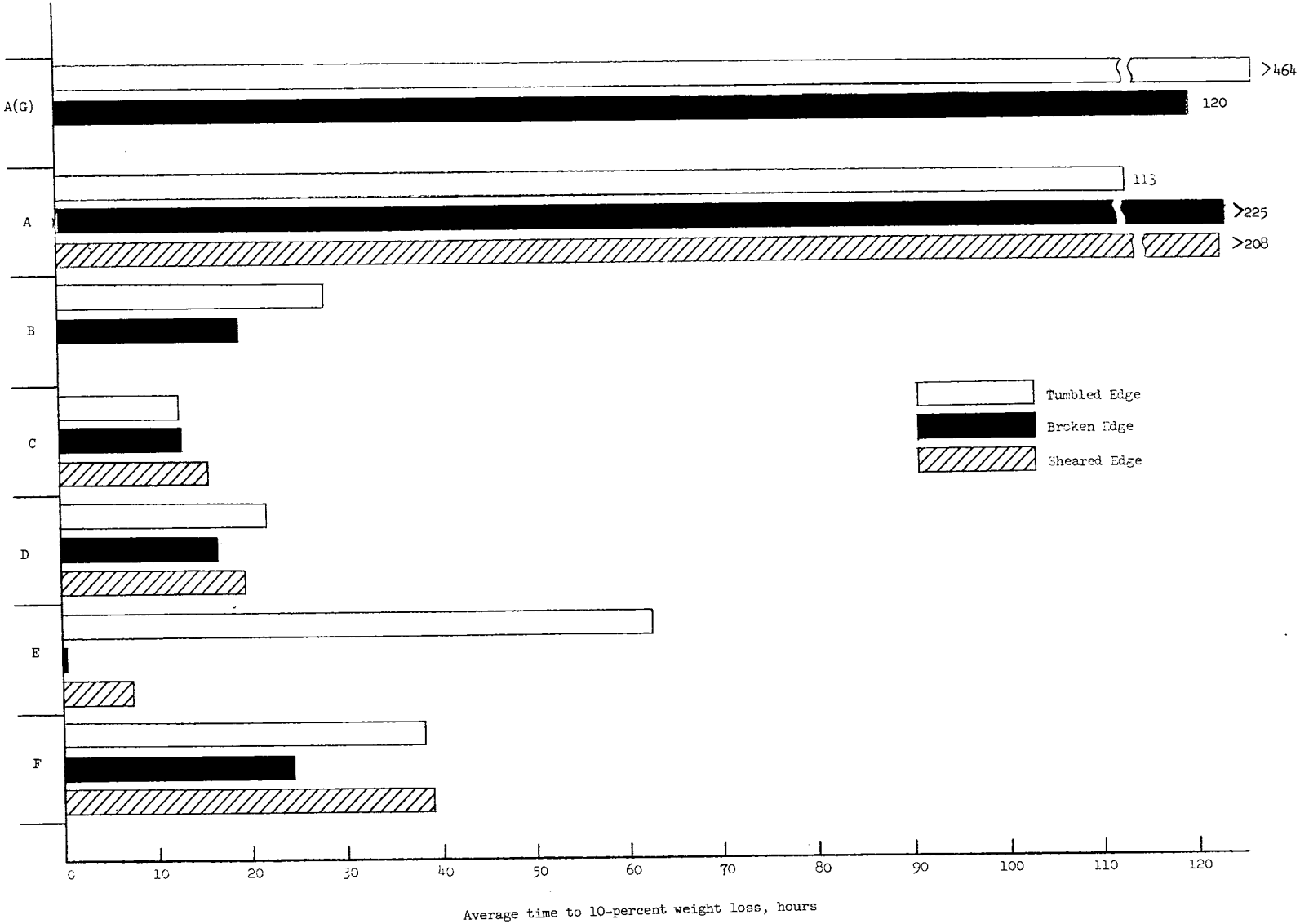

Figure 21.- Continuous-exposure coating life for various edge conditions at 2,500° F.

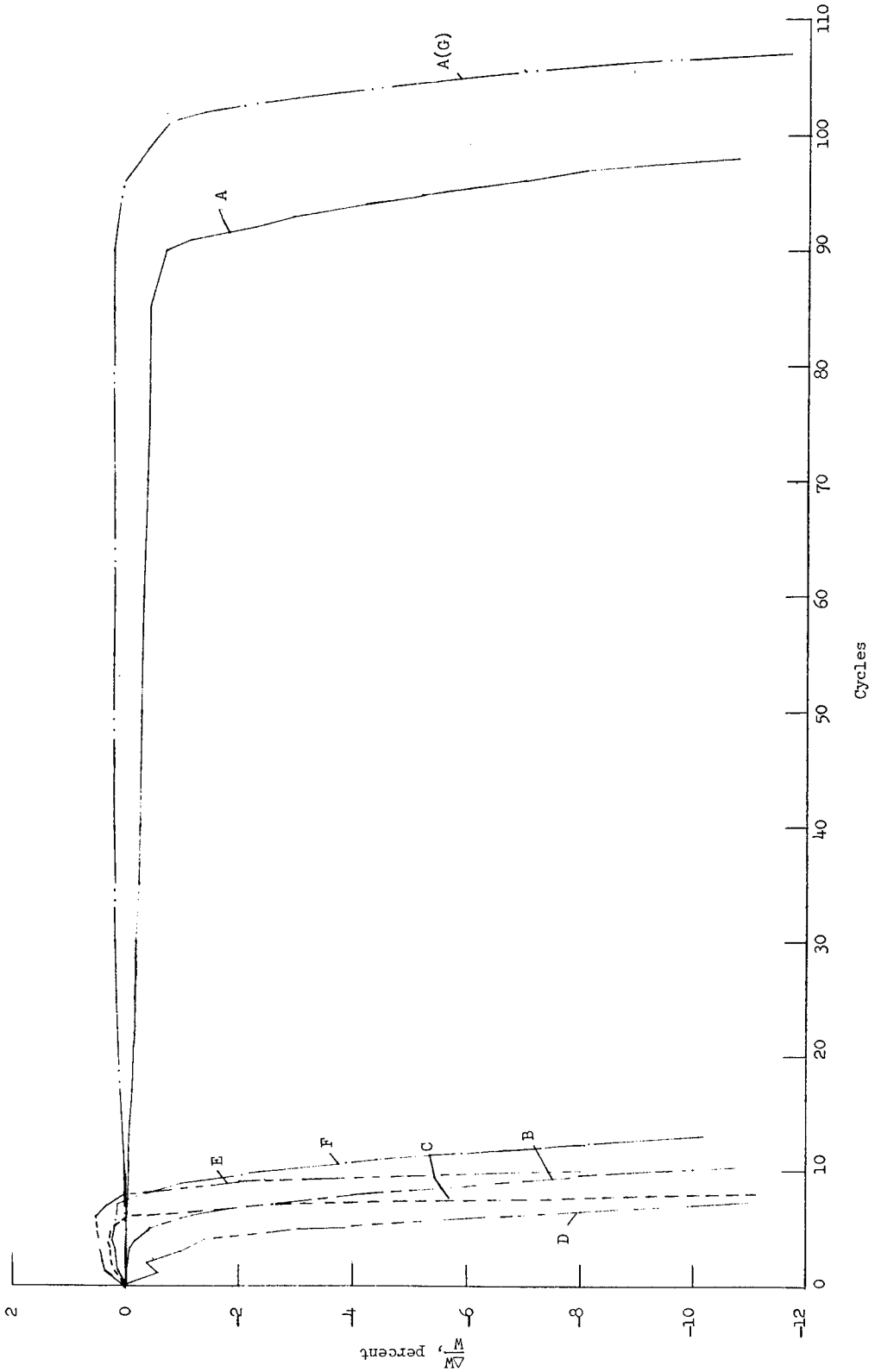

Figure 22.- Typical weight change for 0.1-hour cyclic exposure at 2,500° F for coated Mo-0.5Ti with tumbled edges.

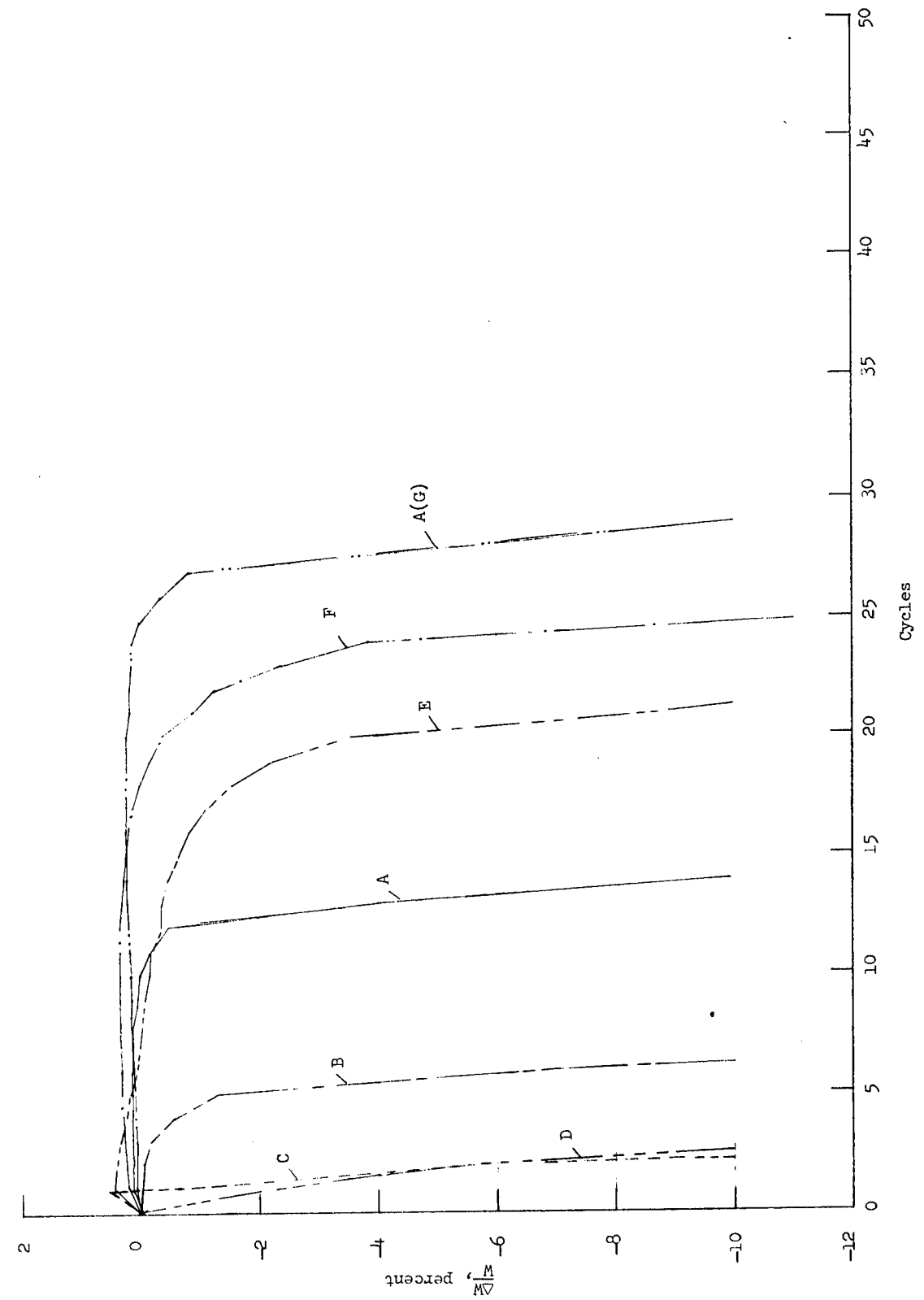

Figure 23.- Typical weight change for 1-hour cyclic exposure at 2,500° F for coated Mo-0.5Ti with tumbled edges.

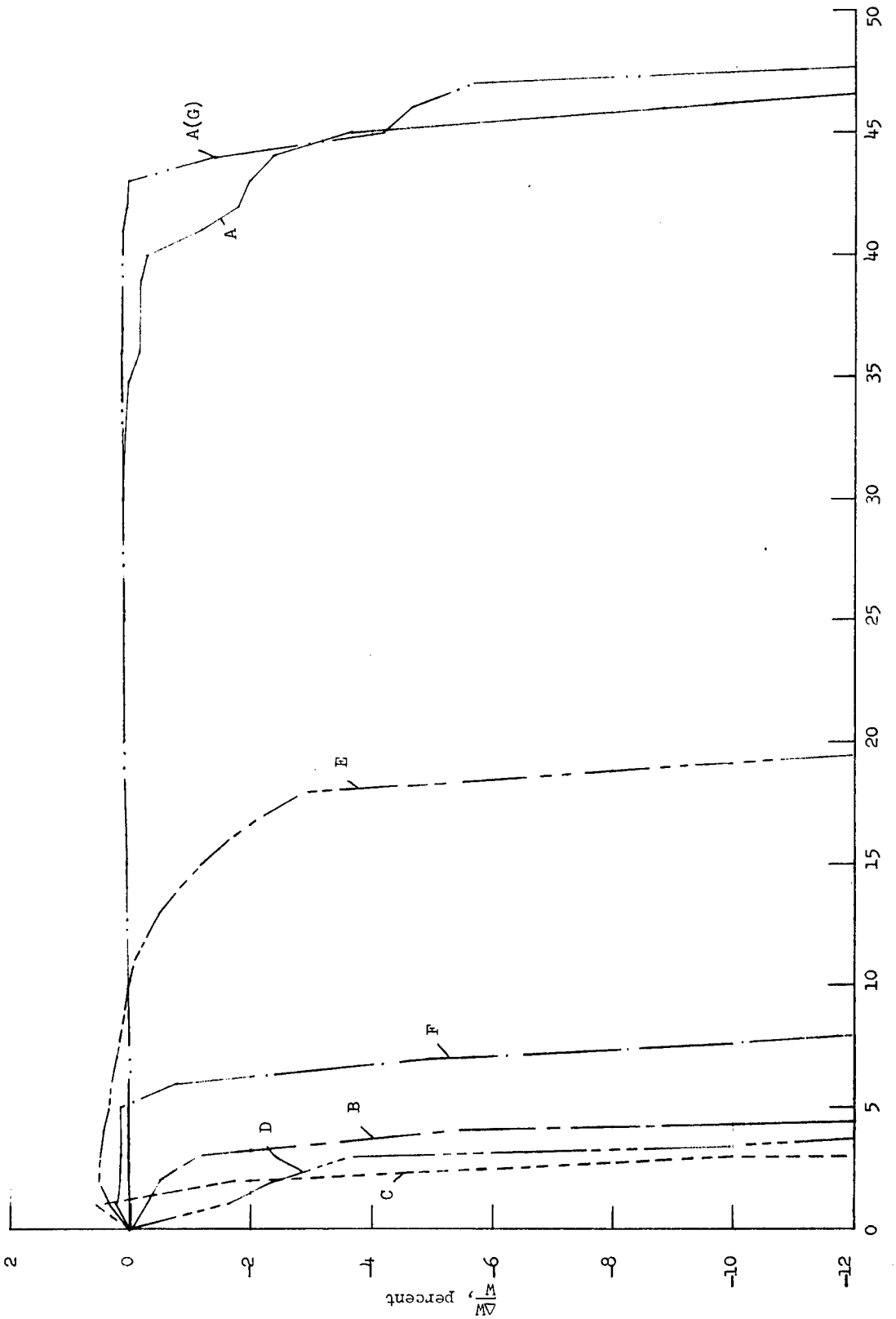

Figure 24.- Typical weight change for 0.5-1.0-0.5-hour cyclic exposure at 2,500° F for coated Mo-0.5Ti with tumbled edges.

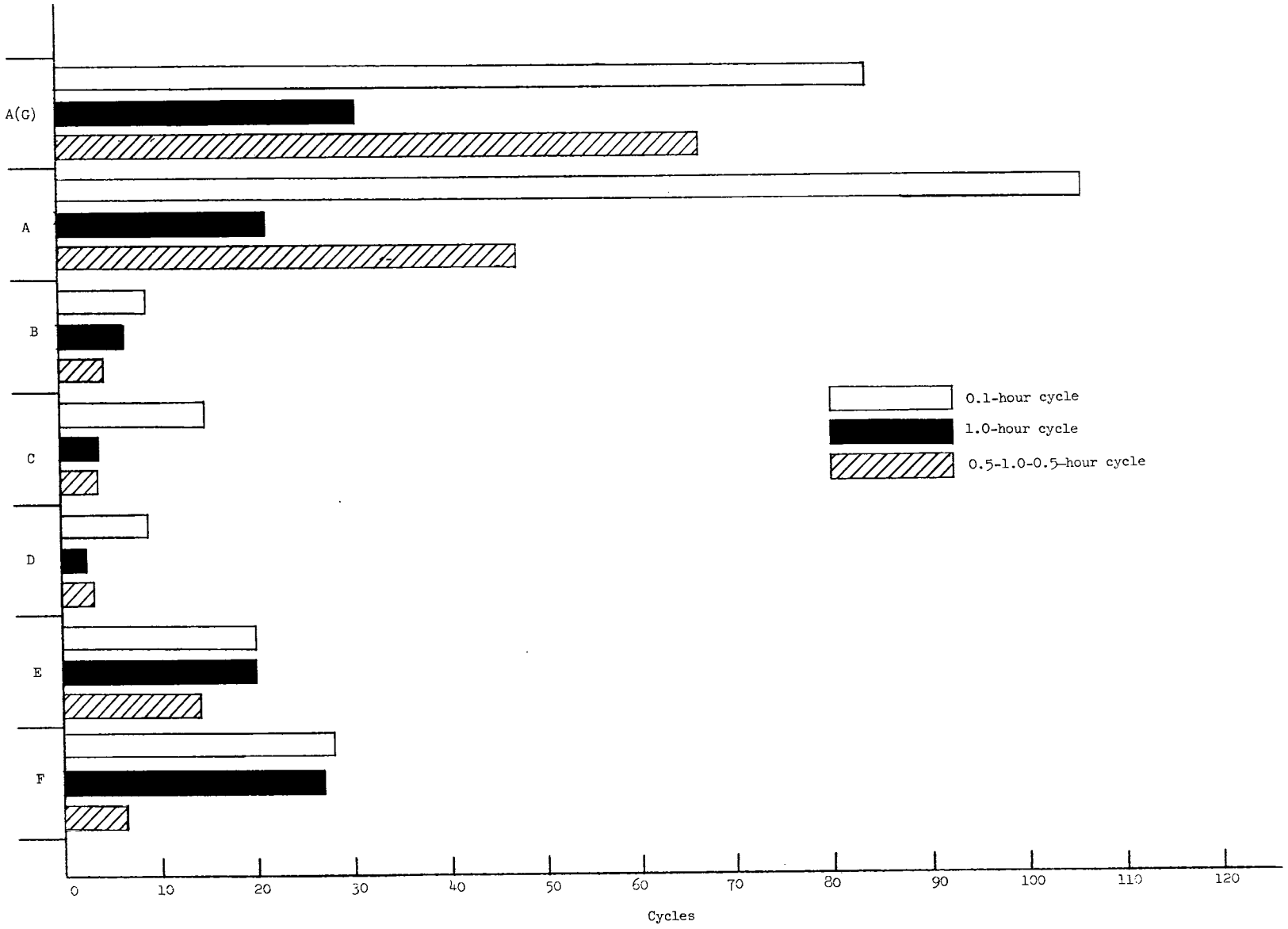

Figure 25.- Average number of cycles to failure (10-percent weight loss) for tumbled-edge specimens at 2,500° F.

(a) Initial defect.

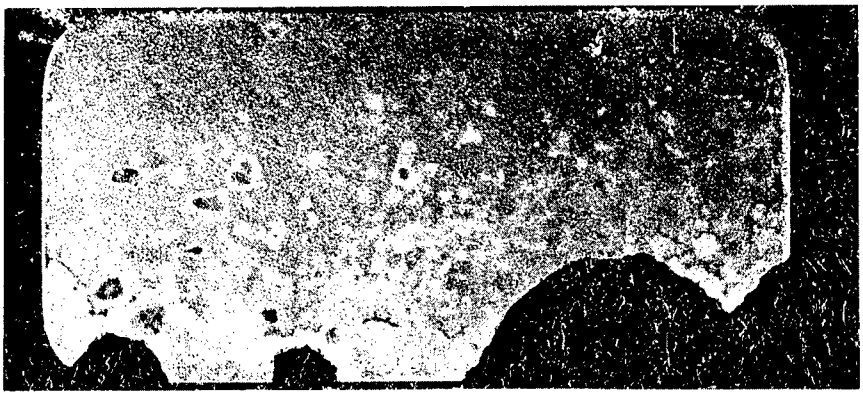

(b) After failure.

L-63-7504

Figure 26.- Coating A tumbled-edge oxidation specimen after 0.1-hour cycles at 2,500° F in air.

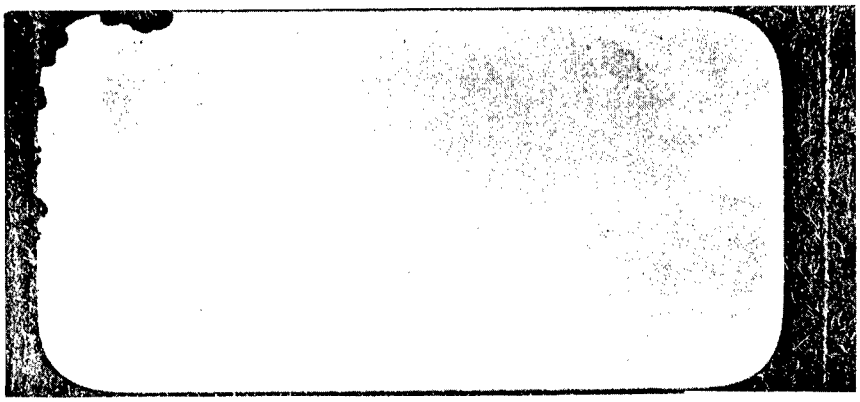

(a) Initial defect.

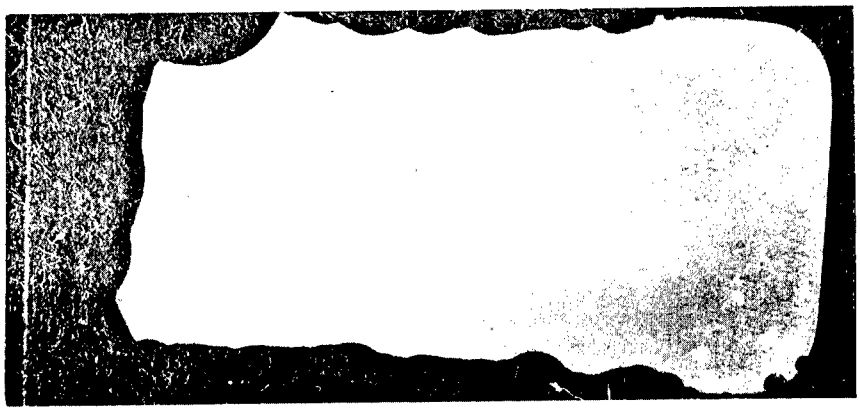

(b) After failure.

L-63-7505

Figure 27.- Coating C tumbled-edge specimen after 0.1-hour cycles at 2,500° F in air.

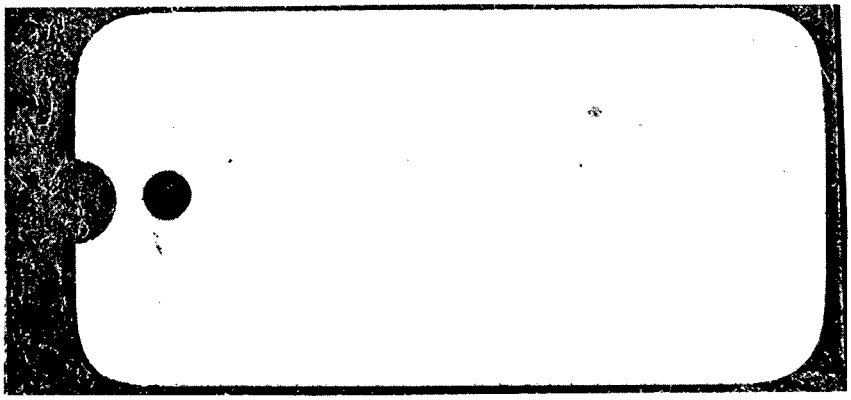

(a) Initial defect.

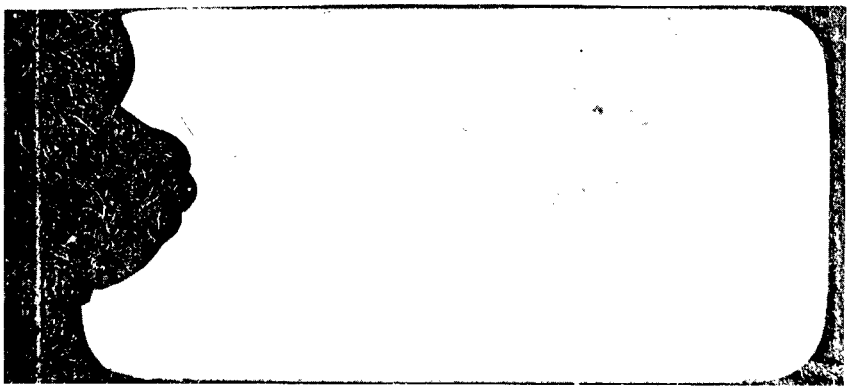

(b) After failure.

L-63-7506

Figure 28.- Coating B tumbled-edge oxidation specimen after 0.1-hour cycles at 2,500° F in air.

(a) Before probing.

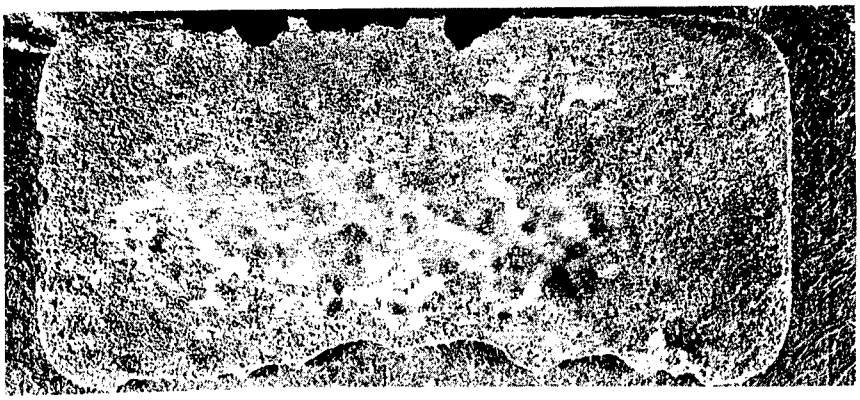

(b) After probing.

L-63-7507

Figure 29.- Coating E tumbled-edge oxidation specimen after forty-four 0.1-hour cycles at 2,500° F in air.

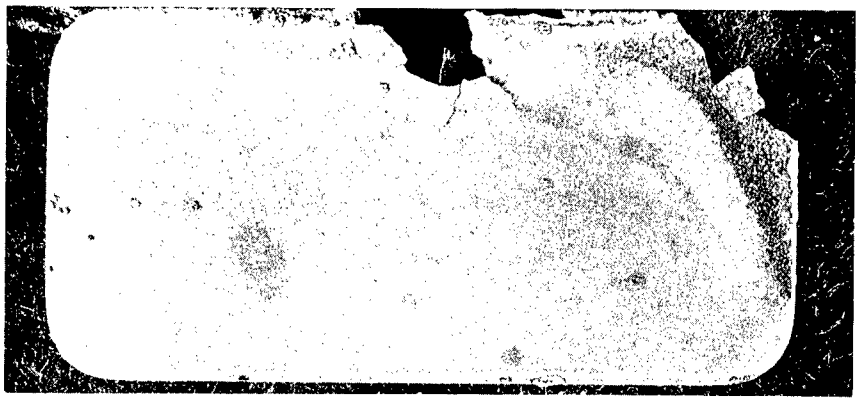

(a) Before probing.

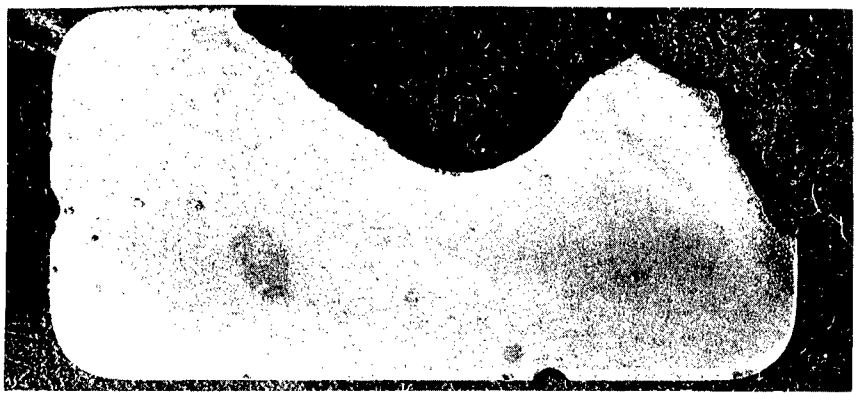

(b) After probing.

L-63-7508

Figure 30.- Coating C tumbled-edge oxidation specimen after three 1.0-hour cycles at 2,500° F in air.

(a) Before probing.

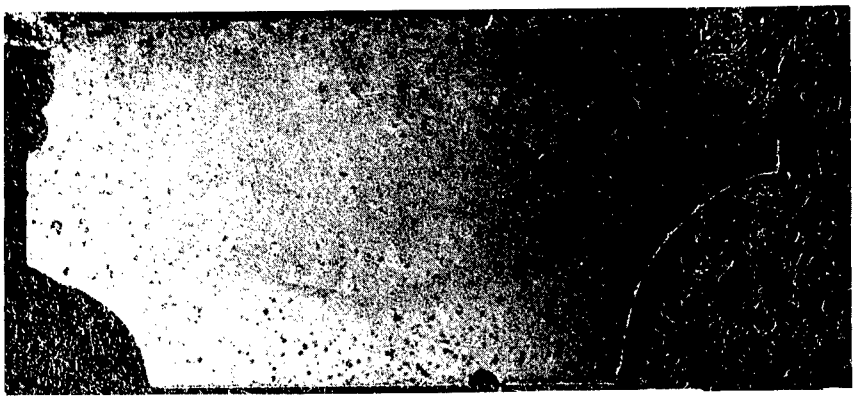

(b) After probing.

L-63-7509

Figure 31.- Coating D tumbled-edge oxidation specimen after four 1.0-hour cycles at 2,500° F in air.

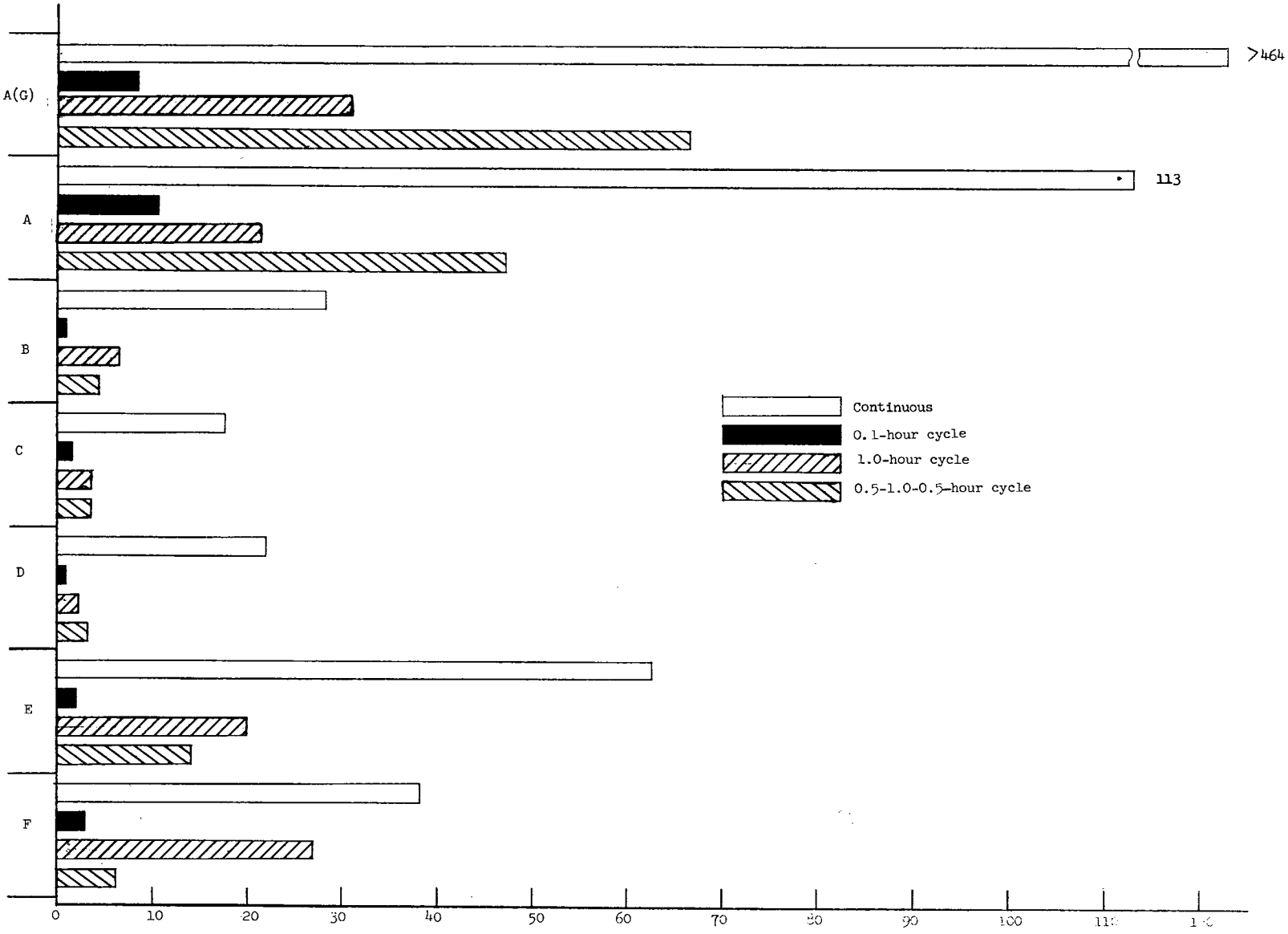

Figure 32.- Comparative results for continuous- and cyclic-exposure tests at 2,500° F.

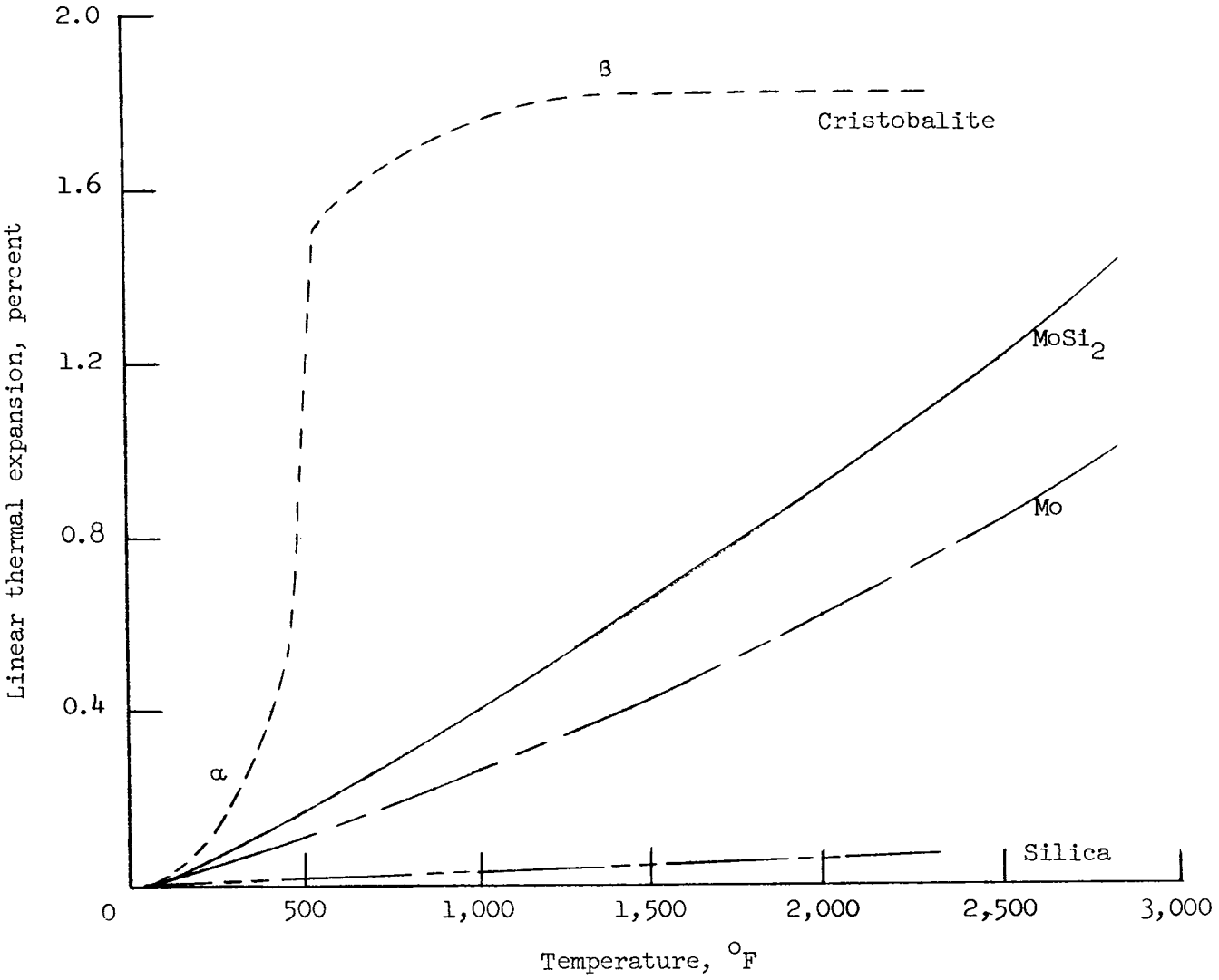

Figure 33.- Linear thermal expansion of selected materials from reference 19.

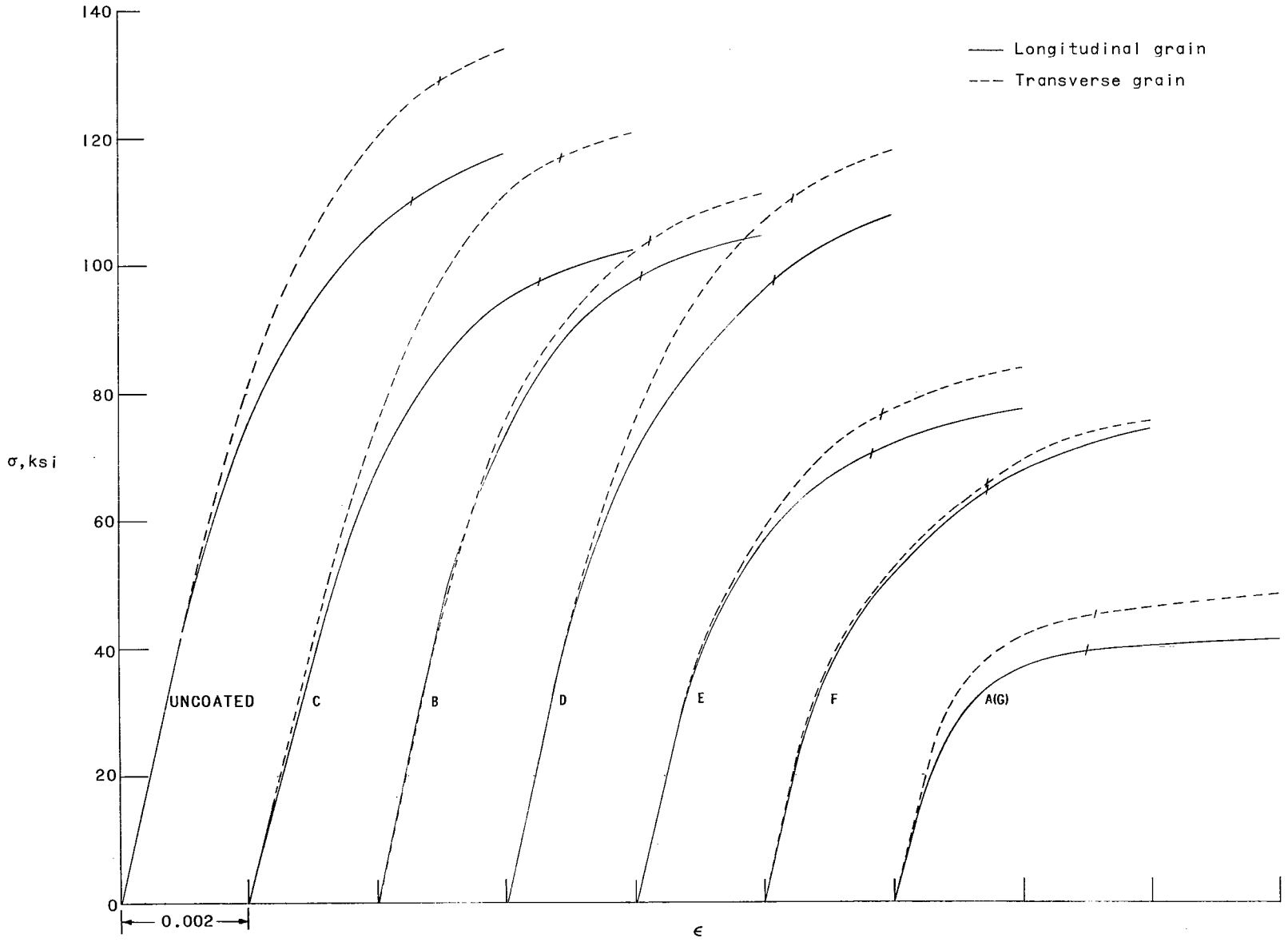

Figure 34.- Typical room-temperature tensile stress-strain curves for Mo-0.5Ti, uncoated and after coating by various suppliers. Stresses are based on specimen areas before coating.

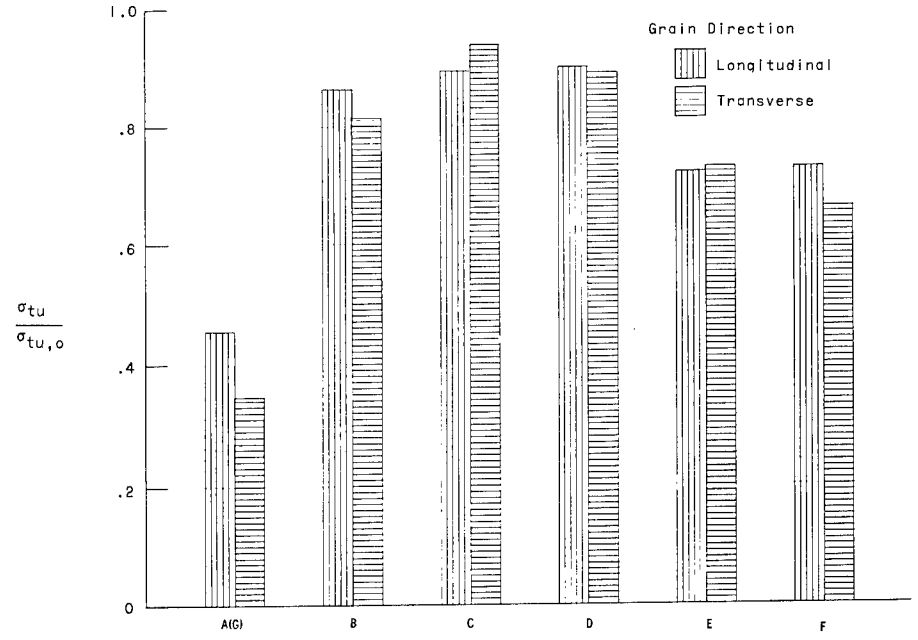

(a) Ultimate strength.

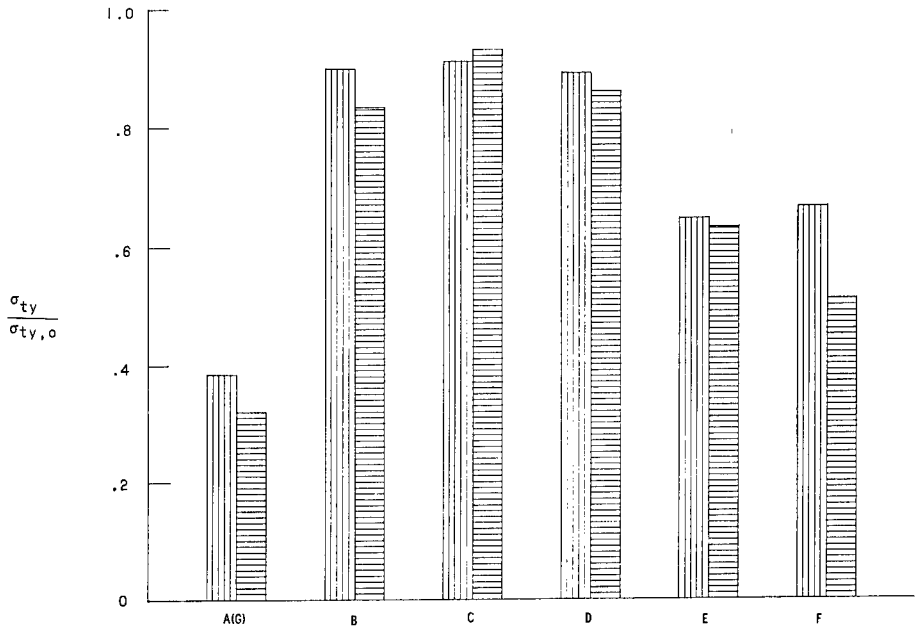

(b) 0.2-percent offset yield stress.

Figure 35.- Ratios of coated to uncoated room-temperature tensile properties of Mo-0.5Ti molybdenum-alloy sheet. Stresses are based on specimen areas before coating.

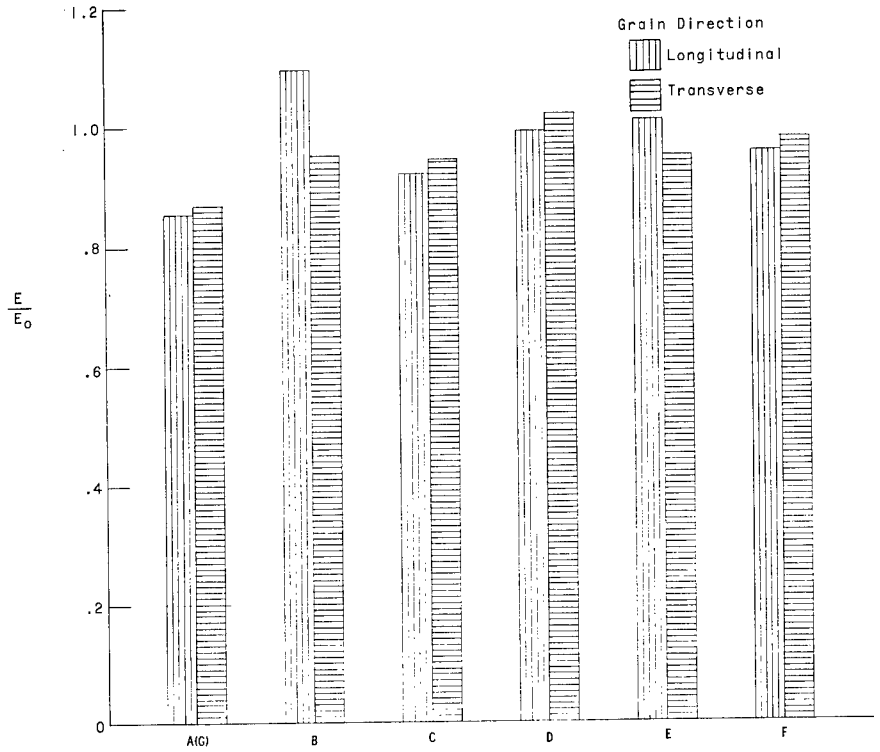

(c) Young's modulus.

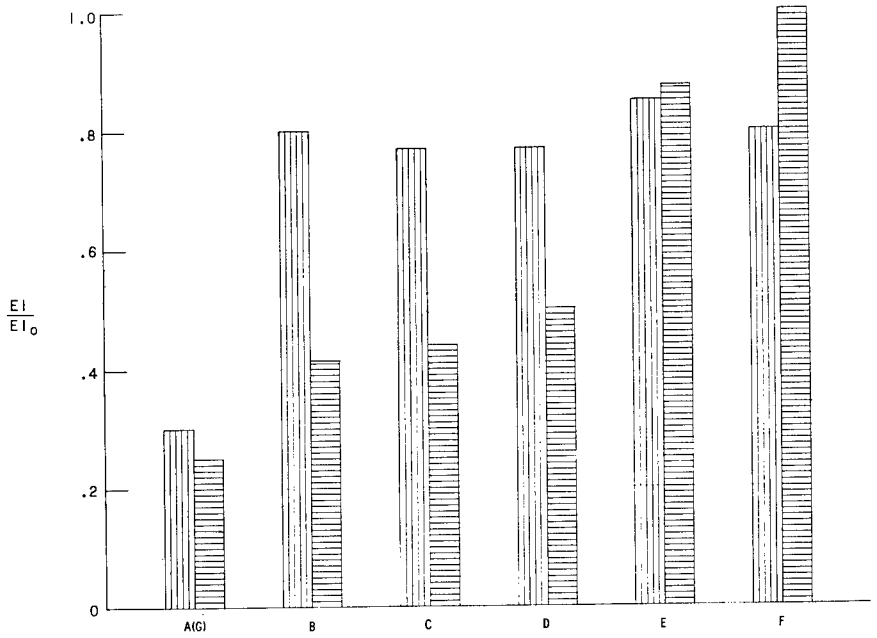

(d) Elongation in 2-inch gage length.

Figure 35.- Concluded.

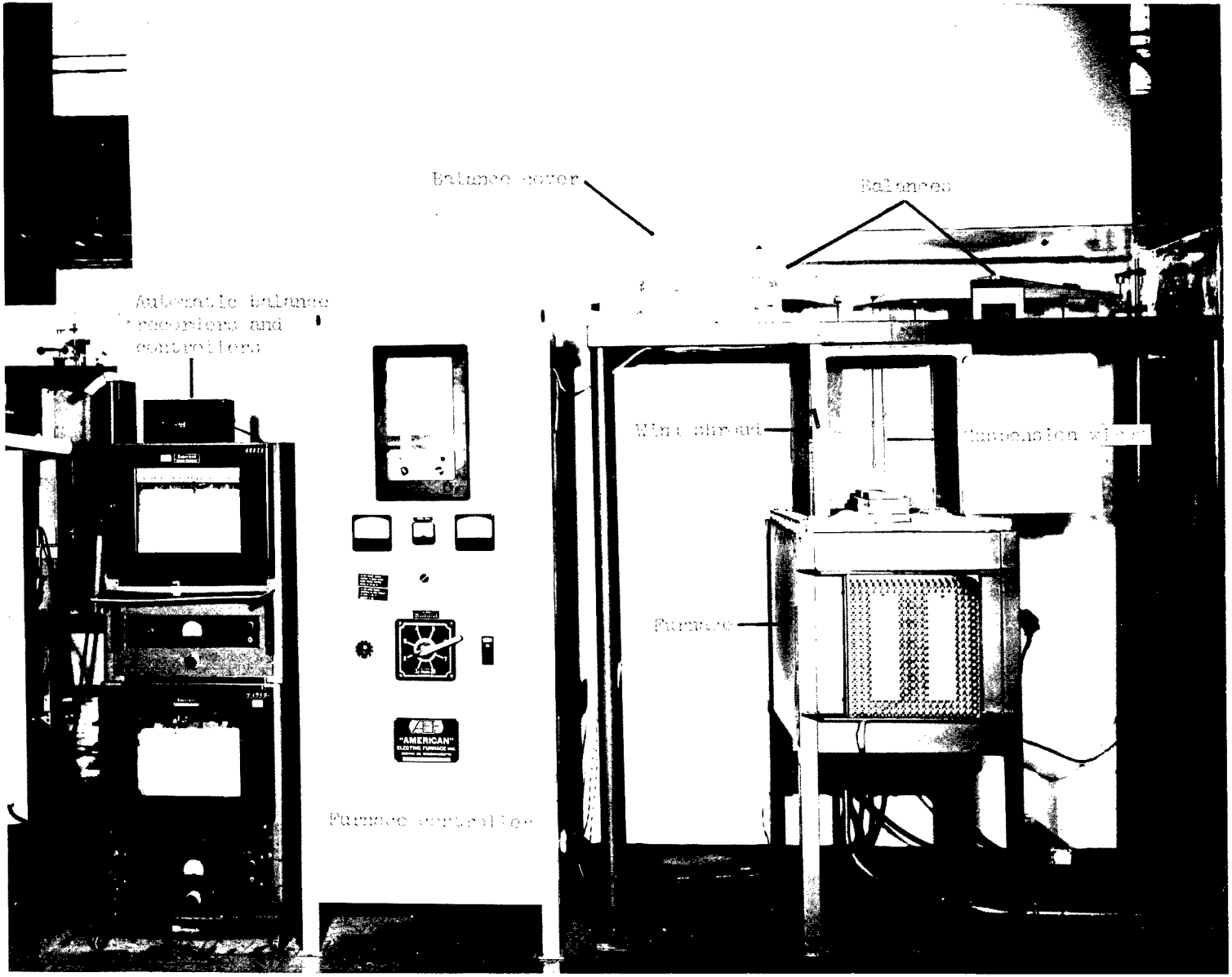

L-63-4394.1

Figure 36.- Vertical tube furnace and associated equipment used for continuous-exposure oxidation tests at 2,500° F in air.

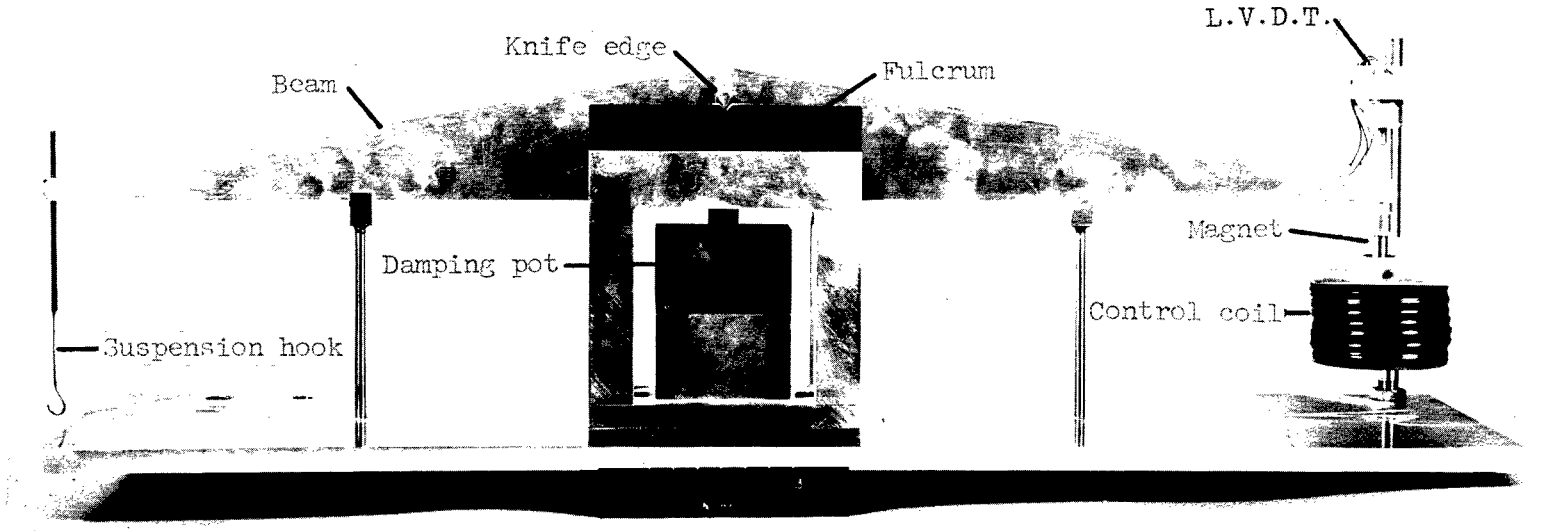

(a) Mechanical details. L-63-4256.1

Figure 37.- Automatic recording balance used for continuous-exposure oxidation tests.

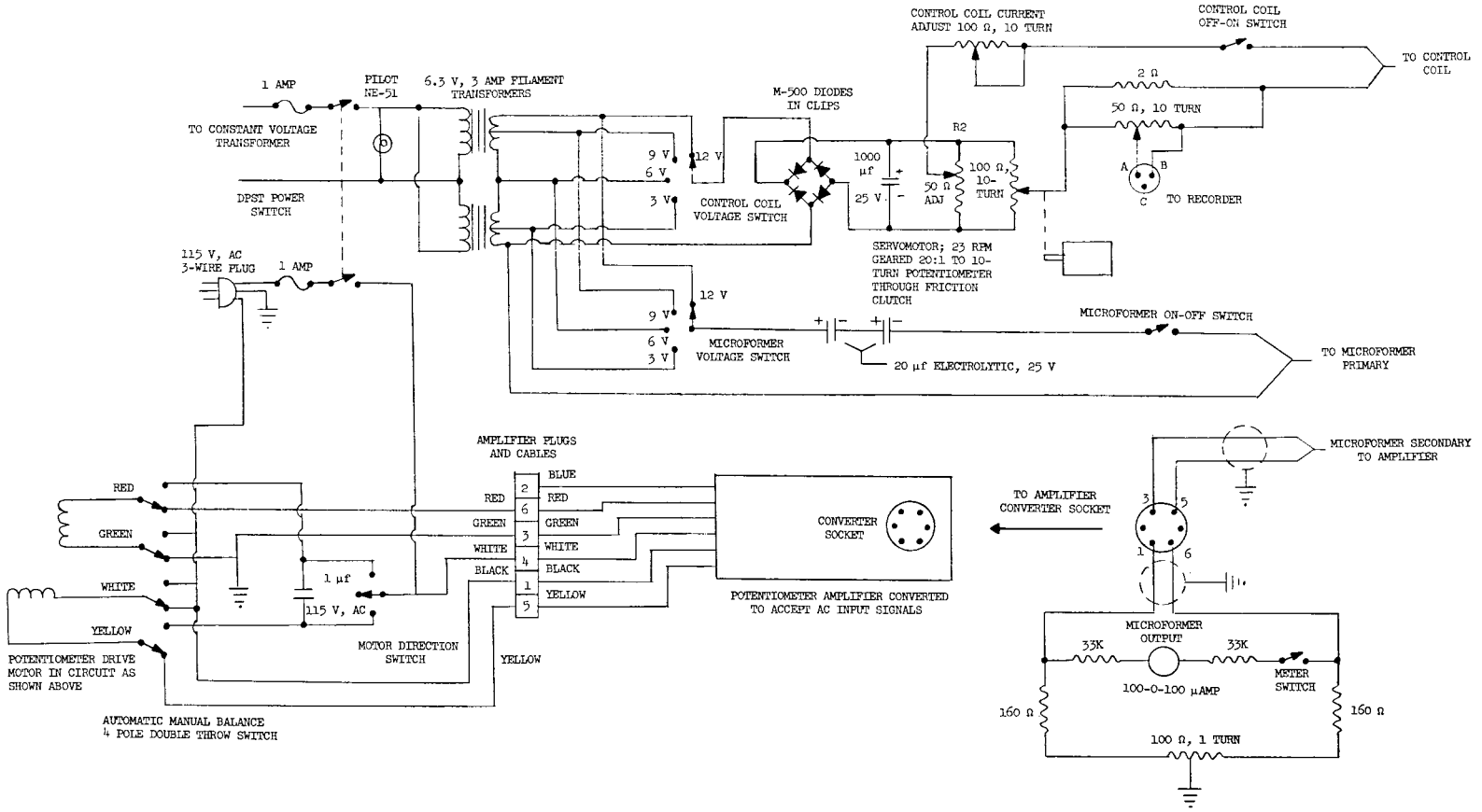

(b) Electrical schematic.

Figure 37.- Concluded.

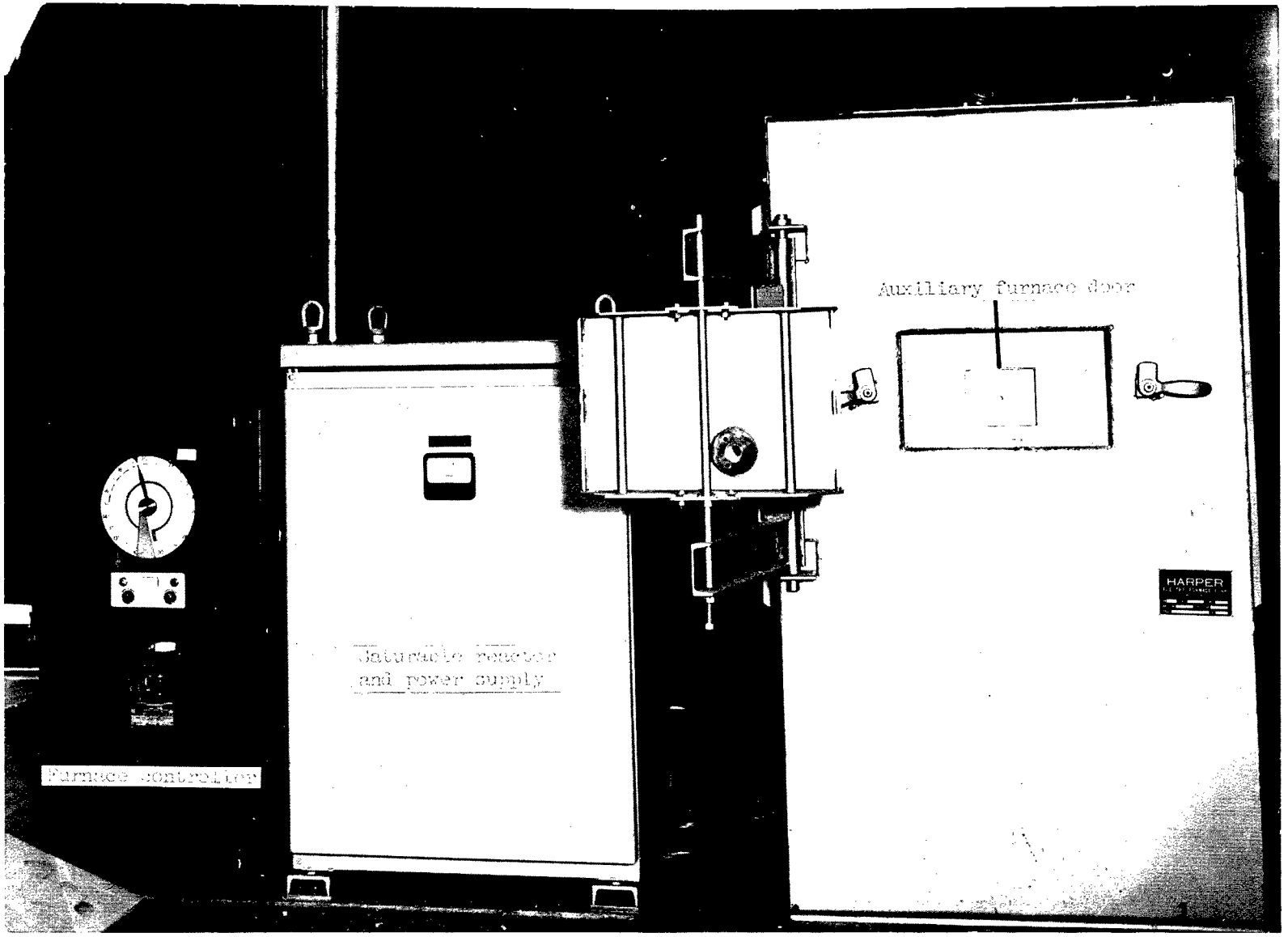

L-61-4972

Figure 38.- Box furnace and associated equipment used for cyclic-exposure oxidation tests at 2,500° F in air.

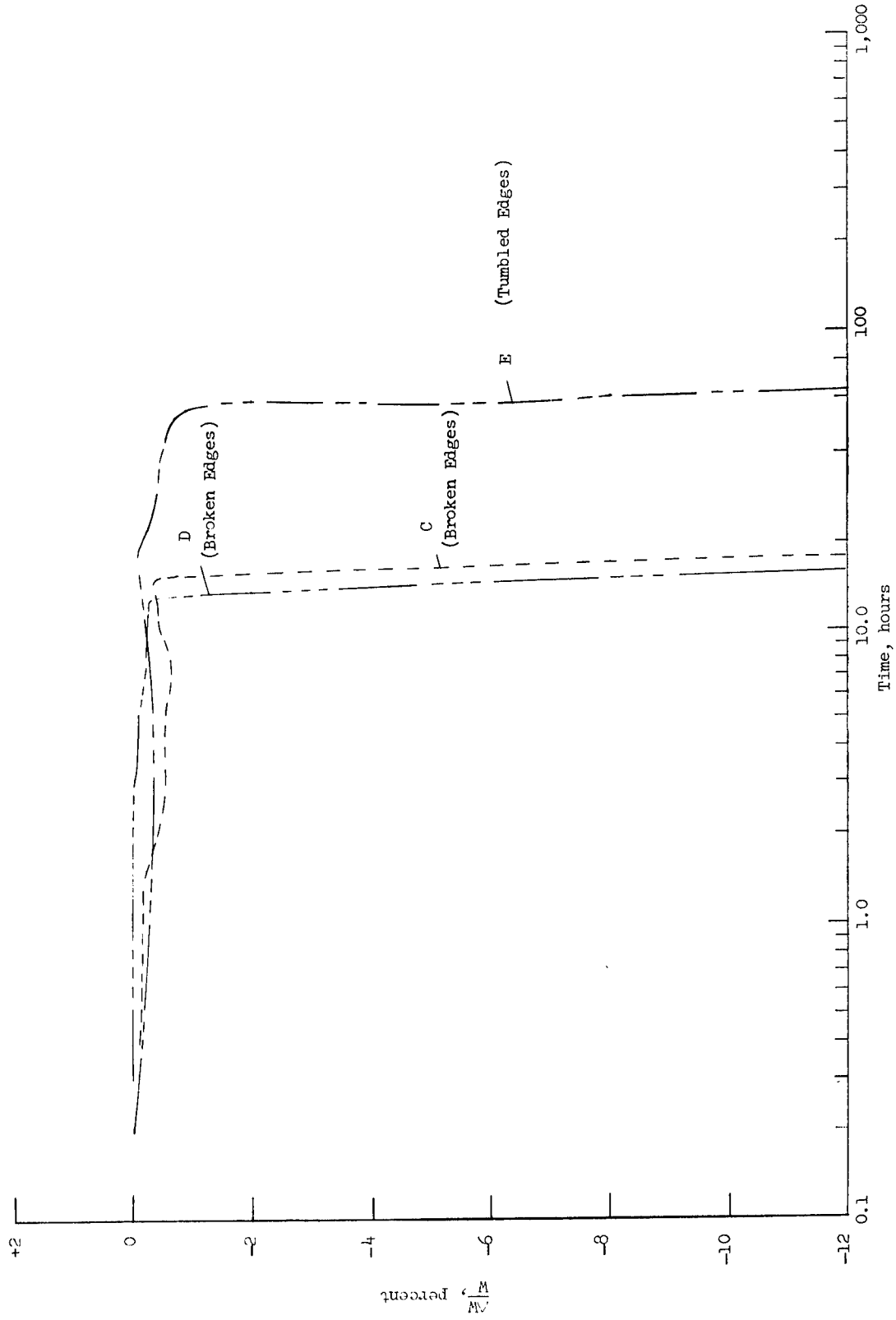

Figure 39.- Typical weight-change plots for continuous exposure at 2,500° F for coated Mo-0.5Ti in box furnace.

NASA-Langley, 1964 L-3406

NASA TN D-2040

temperature mechanical-property tests on the coated specimens.

NASA

NASA TN D-2040

temperature mechanical-property tests on the coated specimens.

NASA

NASA TN D-2040

temperature mechanical-property tests on the coated specimens.

NASA

NASA TN D-2040
National Aeronautics and Space Administration.
A STUDY OF SEVERAL OXIDATION-RESISTANT COATINGS ON Mo-0.5Ti ALLOY SHEET AT 2,500° F. Donald R. Rummler, Bland A. Stein, and Richard A. Pride. August 1964. 78p. OTS price, $2.00.
(NASA TECHNICAL NOTE D-2040)

The results are presented of a study of several silicide-base oxidation-resistant coatings applied to 0.012-inch-thick molybdenum-alloy sheet. The specimens were both continuously and cyclically exposed at 2,500° F in air. The effect of three different types of thermal cycles was investigated. A failure mechanism is proposed to explain the severe reduction observed in the ability of a coating to protect the substrate when thermally cycled. A failure mechanism for the continuously exposed coated specimens is also proposed. The investigation includes the results of X-ray studies and room-
(over)

I. Rummler, Donald R.
II. Stein, Bland A.
III. Pride, Richard A.
IV. NASA TN D-2040

NASA

NASA TN D-2040
National Aeronautics and Space Administration.
A STUDY OF SEVERAL OXIDATION-RESISTANT COATINGS ON Mo-0.5Ti ALLOY SHEET AT 2,500° F. Donald R. Rummler, Bland A. Stein, and Richard A. Pride. August 1964. 78p. OTS price, $2.00.
(NASA TECHNICAL NOTE D-2040)

The results are presented of a study of several silicide-base oxidation-resistant coatings applied to 0.012-inch-thick molybdenum-alloy sheet. The specimens were both continuously and cyclically exposed at 2,500° F in air. The effect of three different types of thermal cycles was investigated. A failure mechanism is proposed to explain the severe reduction observed in the ability of a coating to protect the substrate when thermally cycled. A failure mechanism for the continuously exposed coated specimens is also proposed. The investigation includes the results of X-ray studies and room-
(over)

I. Rummler, Donald R.
II. Stein, Bland A.
III. Pride, Richard A.
IV. NASA TN D-2040

NASA

"The aeronautical and space activities of the United States shall be conducted so as to contribute . . . to the expansion of human knowledge of phenomena in the atmosphere and space. The Administration shall provide for the widest practicable and appropriate dissemination of information concerning its activities and the results thereof."

—NATIONAL AERONAUTICS AND SPACE ACT OF 1958

NASA SCIENTIFIC AND TECHNICAL PUBLICATIONS

TECHNICAL REPORTS: Scientific and technical information considered important, complete, and a lasting contribution to existing knowledge.

TECHNICAL NOTES: Information less broad in scope but nevertheless of importance as a contribution to existing knowledge.

TECHNICAL MEMORANDUMS: Information receiving limited distribution because of preliminary data, security classification, or other reasons.

CONTRACTOR REPORTS: Technical information generated in connection with a NASA contract or grant and released under NASA auspices.

TECHNICAL TRANSLATIONS: Information published in a foreign language considered to merit NASA distribution in English.

TECHNICAL REPRINTS: Information derived from NASA activities and initially published in the form of journal articles.

SPECIAL PUBLICATIONS: Information derived from or of value to NASA activities but not necessarily reporting the results of individual NASA-programmed scientific efforts. Publications include conference proceedings, monographs, data compilations, handbooks, sourcebooks, and special bibliographies.

Details on the availability of these publications may be obtained from:

SCIENTIFIC AND TECHNICAL INFORMATION DIVISION

NATIONAL AERONAUTICS AND SPACE ADMINISTRATION

Washington, D.C. 20546